Journal of Marine Research, 42, 359–393, 1984

Vertical eddy diffusivity in the ocean interior

by A. E. Gargett[1]

ABSTRACT

Vertical turbulent transport of density (mass) in a system of stable stratification $\partial\rho/\partial z < 0$ (z positive upward) is often modelled by an "eddy" diffusivity $K_\nu \equiv -\overline{\tilde{\rho}w}/(\partial\rho/\partial z)$, normally assumed to be constant. Recent evidence from stratified lakes, fjords and oceans suggests that K_ν may be more accurately described as a decreasing function of buoyancy frequency $N \equiv (-g(\rho_o)^{-1}(\partial\rho/\partial z))^{1/2}$. A main purpose of this paper is to review available estimates of K_ν from a variety of stratified geophysical systems. Particular emphasis is placed upon the degree to which these estimates are dependent upon underlying models used to derive values for K_ν from observable quantities. Most techniques reveal a disagreeable degree of model-dependence, frequently providing only upper bounds to the magnitude of K_ν. I have coupled the functional dependence which emerges from the least model-dependent of available techniques with ensemble-averaged values of oceanic turbulent kinetic energy dissipation rate per unit mass ϵ as a function of N, and show that the resulting parameterization for K_ν is consistent with a wide range of present oceanic data. Finally, brief re-examination of a simple vertical advection/diffusion model of thermohaline circulation illustrates possible dynamical significance of a stratification-dependent K_ν.

1. Introduction

The vertical turbulent transport of density in a system of mean stratification $\partial\rho/\partial z$ is regularly modelled as Fickian diffusion characterized by diffusivity $K_\nu \equiv -\overline{\tilde{\rho}w}/(\partial\rho/\partial z) \gg D$, where $\overline{\tilde{\rho}w}$ is vertical turbulent density flux and D is an effective molecular diffusivity for density. Equally regularly, it is assumed that K_ν is a constant. However, recent evidence from a variety of stratified geophysical systems (lakes, fjords and oceans) suggests that K_ν is *not* constant, but a decreasing function of buoyancy frequency $\mathrm{N} \equiv (-g(\rho_o)^{-1}(\partial\rho/\partial z))^{1/2}$, a measure of vertical stability (vertical restoring force). Recognition of the degree of order amidst estimates of K_ν from widely differing stratified regimes led to a recent suggestion (Gargett and Holloway, 1984: henceforth referred to as GH) that all systems in which energy reaches dissipation ("turbulent") scales via the intermediary of internal waves should exhibit N-dependent averaged values of the kinetic energy dissipation rate ϵ and of K_ν. A brief review of the GH arguments is provided in Section 2, to clarify both the type of system considered and the degree of averaging implied in the previous statement.

1. Institute of Ocean Sciences, Patricia Bay, P.O. Box 6000, Sidney, B.C., Canada, V8L 4B2.

A number of recent reviews have compiled estimates of K_ρ derived from a range of experimental data (Garrett, 1979; Gregg and Briscoe, 1979; Caldwell, 1983). In Section 3, I re-examine the approximations and assumptions underlying the major techniques for estimating K_ρ, with the aim of discovering which of these results are most trustworthy. Based on the latter, Section 4 suggests a form for the oceanic K_ρ due to internal wave breaking, while Section 5 presents a more speculative discussion of possible implications of an N-dependent K_ρ.

2. N-dependence of K_ρ

GH consider stably-stratified systems which are not unstable to double-diffusion and in which kinetic energy resides dominantly in internal wave motions. As examples, these motions might be internal seiches generated by the action of wind on the surface of a lake or fjord, internal waves generated by tidal flow over sills in fjords or oceans, or the multi-wave field of the ocean interior. Subsequent analysis requires that the wave kinetic energy be steady-state: thus the averaging time chosen must include many generation events for the particular wave field in question. For the examples mentioned above such an averaging time would include respectively many seiche-generating wind events, or many tidal periods, or many of the events (wind events generating inertial waves?) responsible for maintaining the oceanic internal wave field. Derived quantities such as ϵ and K_ρ are thus implicitly thought of as values averaged over the same time. Two additional assumptions are (i) that the flux Richardson number

$$R_f \equiv \frac{-g\overline{\tilde{\rho} w}}{\overline{\left(u_i w \frac{\partial u_i}{\partial z}\right)}}; i = 1, 2$$

is small ($R_f \ll 1$) and nearly constant, and (ii) that the internal wave motions are Richardson-number limited in the sense that

$$Ri_w \equiv \frac{N^2}{\overline{\left(\frac{\partial u_i}{\partial z}\right)^2}_w} = \frac{N^2}{\int_o^{k_u} \phi_s \, dk} \sim 0(1),$$

where k_u, the upper limit of the integral over shear spectral density ϕ_s, lies below dissipation wavenumbers, i.e. $k_u \gtrsim 1/30\ k_s$, $k_s \equiv (\epsilon/\nu^3)^{1/4}$ (Gibson and Schwartz, 1963). The first assumption enjoys considerable support from both laboratory and field experiments, while the second may be thought of as a generalized stability condition for a stratified shearing flow, coupled with a very loose distinction between waves and turbulence on the basis of their dissipative properties (more detailed discussion of both

assumptions may be found in GH). Examining the kinetic energy equation for a system with the above characteristics, GH argue that

$$\epsilon = T_o \left[\overline{u_i^2}\ \overline{w^2} \overline{\left(\frac{\partial u_i}{\partial z} \right)_w^2} \right]^{1/2} \tag{1}$$

and

$$K_v = \frac{R_f}{1 - R_f} \epsilon N^{-2}, \tag{2}$$

where T_o is a nondimensional triple correlation coefficient. From assumption (ii) above, $\overline{(\partial u_i/\partial z)_w^2} \sim N^2$, so that a functional form for ϵ (hence K_v) depends upon the N-dependence of the internal wave velocity variances $\overline{u^2}$ and $\overline{w^2}$. Two extreme cases are identified:

Case (1): Waves of a (nearly) single frequency have $\overline{u^2} \sim N$ and $\overline{w^2} \sim N^{-1}$; hence $\epsilon \sim N^{+1}$ and $K_v \sim N^{-1}$.

Case (2): The broad-band oceanic internal wave spectrum GM79 (Munk, 1981), in which bandwidth as well as amplitude varies with N, has $\overline{u^2} \sim N$ and $\overline{w^2} \sim$ const.; hence $\epsilon \sim N^{+1.5}$ and $K_v \sim \mathrm{N}^{-0.5}$.

In summary, GH suggest that relations of the form

$$\epsilon = \epsilon_o N^{+p} \tag{3}$$

and

$$K_v = \frac{R_f \epsilon_o}{(1 - R_f)} N^{-2+p} = a_o N^{-q} \tag{4}$$

where $1.0 \leq p \leq 1.5$ (hence $0.5 \leq q \leq 1.0$) and $R_f \simeq 0.20$, should be characteristic of systems in which diapycnal mixing results from internal wave breakdown to "turbulence."

The values of the "constants" ϵ_o and a_o will be site-specific, since they depend upon the actual amount of energy in a particular internal wave field, as well as the magnitude of the nondimensional triple correlation coefficient T_o (Eq. (1)), presumably a measure of the efficiency of any particular breakdown mechanism. Viewed this broadly, the relations (3) and (4) may be imagined to hold whether internal wave motions lose their energy by breaking within the body of a system (interior mixing) or along its boundaries (edge mixing): what *is* important is that the variances which enter (1) be associated with an internal wave field and not some space-time "mean" velocity field; i.e., one which does not scale locally with N.

3. Observational evidence

All existing estimates of vertical turbulent eddy diffusivity K_v for geophysical stratified systems have been obtained through budgets for either c, the "mean" concentration of a dynamically passive scalar, or $\overline{(c')^2}$, the fluctuation variance of this scalar. Various methods of employing these budgets can be model-dependent to a greater or lesser degree, and the extent of such dependence is crucial to evaluating the nature of the resulting estimates of K_v. Both equations are briefly re-stated here in order to provide a framework for viewing the further assumptions necessary to use them for estimating K_v.

Consider a rectangular coordinate system $(x_1, x_2, x_3) = (x, y, z)$, with x eastward, y northward, z in the direction of local vertical, and zero at the sea floor. Let $(U_1, U_2, U_3) = (U, V, W)$ be an incompressible velocity field which advects scalars. Then the law of conservation of a scalar quantity C per unit mass is given by

$$\frac{\partial C}{\partial t} + U_i \frac{\partial C}{\partial x_i} = \frac{\partial}{\partial x_i}\left(D_c \frac{\partial C}{\partial x_i}\right) + F$$

where D_c (assumed constant) is the molecular diffusivity of the scalar C, and F is an *in-situ* source (sink) of C (Monin and Yaglom, 1971: Sec. 1.5). Note that C may represent concentration of a radio-active scalar provided either (i) C is taken as decay-corrected concentration or (ii) decay is included specifically as a sink term proportional to concentration. Separating the scalar and velocity fields into mean and fluctuating parts by choosing an averaging procedure (overbar) such that with $C = c + c'$ and $U_i = u_i + u_i'$, $\overline{C} = c$ and $\overline{U_i} = u_i$, the equation for conservation of mean scalar concentration becomes

$$\frac{\partial c}{\partial t} = -u_i \frac{\partial c}{\partial x_i} - \overline{u_i' \frac{\partial c'}{\partial x_i}} + \frac{\partial}{\partial x_i} D_c \frac{\partial c}{\partial x_i} + F \tag{6}$$

(Monin and Yaglom, 1971: Sec. 5.1).

When the incompressibility condition $\partial u_i/\partial x_i = 0$ is used to rewrite the second term on the right-hand side in a divergence form similar to the third,

$$\overline{-u_i' \frac{\partial c'}{\partial x_i}} = \frac{\partial}{\partial x_i}\left(\overline{-u_i' c'}\right)$$

it is clear why it is tempting to define a second-order "turbulent" diffusion tensor K_{ij} by the relationship $K_{ij}\, \partial c'/\partial x_j \equiv \overline{-u_i' c'}$, thus modelling the effects of "turbulence" as an enhanced (i.e. $|K_{ij}| \gg D_c$) but nonetheless Fickian diffusion.

This model has proven a reasonable one for passive scalars in turbulent flows characterized by single "turbulent" length and velocity scales (Tennekes and Lumley,

1972). However, in stratified geophysical systems, typical vertical and horizontal length scales differ, and the diffusivity tensor is generally chosen to have the form

$$K_{ij} = \begin{pmatrix} K_x & 0 & 0 \\ 0 & K_y & 0 \\ 0 & 0 & K_v \end{pmatrix}$$

with $0 < D_c \ll K_v \ll K_x \sim K_y$. This choice represents a minimum of complexity (i.e., no cross-terms) consistent with the prevalent belief that "turbulent" processes producing vertical transports are different from those producing horizontal transports.[2] With these assumptions, Eq. (6) becomes:

$$\frac{\partial c}{\partial t} = -u_i \frac{\partial c}{\partial x_i} + \frac{\partial}{\partial x_i}\left(K_{ij} \frac{\partial c}{\partial x_j}\right) + F. \tag{7}$$

Using the same form for $\overline{(u_i'c')}$ and defining $0 < \chi_c \equiv 2D_c\overline{(\partial c'/\partial x_i)^2}$ as the dissipation rate of $\overline{(c')^2}$, the conservation equation for scalar fluctuation variance is

$$\frac{\partial}{\partial t}\overline{(c')^2} = -u_i \frac{\partial}{\partial x_i}\overline{(c')^2} - \frac{\partial}{\partial x_i}\overline{u_i'(c')^2} + 2K_{ij}\frac{\partial c}{\partial x_i}\frac{\partial c}{\partial x_j} - \chi_c \tag{8}$$

(Monin and Yaglom, 1971: Sec. 6.2).

One of Eqs. (7) and (8), describing respectively the conservation of either c or $\overline{(c')^2}$, forms the starting point for every method presently used to determined K_v from observations. I have grouped these methods into three categories: (a) budget methods in closed basins and (b) models of mean-scalar balance both employ Eq. (7), while (c) models of scalar-variance balance use Eq. (8). The budget methods (a) are considered separately because, when carefully applied, they are much less model-dependent than either (b) or (c), hence produce the most tightly constrained estimates of K_v. The following discussion of each method will outline further assumptions which are made in order to derive values for K_v, then illustrate the method with representative and/or recent examples.

a. Budget models

For a stratified fluid contained in a closed basin, the mean-scalar conservation equation (7) may be simplified considerably by integrating over the horizontal extent of the basin at any depth and assuming boundary conditions of no flow and no scalar flux through solid boundaries (depending upon the scalar in question, the scalar flux

2. Since typical mean isopycnal slopes in geophysical systems are small, I shall use the term "vertical" to imply "diapycnal" (cross-isopycnal) and "lateral" (horizontal) to imply "isopycnal" (along-isopycnal). This identification is correct to order α^2, where $\alpha \ll 1$ is the angle between an isopycnal surface and local horizontal (Sarmiento and Rooth, 1980). Lateral mixing processes do not by definition affect the distribution of ρ, but do affect distribution of any scalar which has gradients along isopycnals.

condition must be carefully considered: for the moment I assume it is valid). Using a tilde to denote the horizontal average, Eq. (7) becomes

$$\frac{\partial \tilde{c}}{\partial t} = -\frac{\partial}{\partial z}(\widetilde{wc}) + \frac{\partial}{\partial z}\left(K_v \frac{\partial \tilde{c}}{\partial z}\right) + \tilde{F}. \tag{9}$$

Integrating from the bottom boundary at $z = 0$ to height z, Eq. (9) can be solved for

$$K_v(z) = \frac{\left\{\frac{\partial}{\partial t}\left[\int_o^z \tilde{c}\, dz\right] + \widetilde{wc}\,|_o^z - \int_o^z \tilde{F}\, dz\right\}}{\frac{\partial \tilde{c}}{\partial z}} \tag{10}$$

in terms of quantities which are either zero or measurable in many situations.

Eq. (10) has been used by a number of authors to analyze observations from stratified lakes and from deep waters of sill-fjord estuaries. Both are systems in which $\widetilde{wc} = 0$ at all times (lakes) or for extended periods of time (deep water renewal in sill-fjord estuaries is sporadic, short-lived and normally occurs in winter). Both are systems in which internal mixing (below any wind-mixed surface layer) is believed to be dominated by the breakdown of internal waves, whether internal seiches generated by the action of wind on the water surface (lakes and fjords) or internal waves generated by tidal flow over sills (fjords). Advantages of the budget method are twofold: first, a minimum of additional assumptions enter Eqs. (9) and (10) and second, considerable (time-) averaging is implicit in deriving $K_v(z)$ from measurements of the time rates of change of scalar concentrations and gradients. Such averaging is essential for systems in which turbulent mixing occurs sporadically.

The first application of (10) was that of Jassby and Powell (1975), who examined the heat budget for Castle Lake during a three-month summer period when the lake was stably stratified by temperature. Identifying the scalar c as temperature T, Jassby and Powell measured $\partial T/\partial z$ and

$$\frac{\partial}{\partial t}\left[\int_o^z \tilde{T}\, dz\right]$$

and estimated the *in-situ* source term (due to solar heating) by measuring incident solar radiation at the water surface and distributing it with depth as a function of the sun's zenith angle. Averaged over the 3-month period, their results show a well-defined minimum of K_v in the thermocline of the lake, followed by an increase with increasing depth (decreasing N). Fitting all of their data to a form $K_v = a_o N^{-q}$ using a weighted least-squares algorithm gave $q = +0.8 \pm 0.04$.

Further application of the heat budget approach is reported by Quay *et al.* (1980), who carried out a similar calculation for a temperature-stratified lake (L224) in the Experimental Lakes Area (ELA) of northwestern Ontario. For the entire stratified

season of 1976, their measurements yielded $K_\nu \alpha N^{-q}$ with $q = 0.92 \pm 0.06$. The similarity of this expression to that obtained by Jassby and Powell led them to determine K_ν and N for 10 other ELA lakes; of these, 6 showed a statistically significant relation of the form $K_\nu \alpha N^{-q}$, with an average $q = 0.88 \pm 0.16$. They also report similar heat budget calculations yielding $q = 0.90$ for both Lake Washington (Quay, unpublished) and Lake Zurich (Li, 1973). Thus available heat budget results from lakes appear to be internally consistent[3]; the resulting values of K_ν clearly depend upon an inverse power of N. The accuracy of the determination of the exponent q depends mainly upon the assumption of zero boundary heat flux. Jassby and Powell simply neglect this effect, while Quay *et al.* carry out a rough estimate of error caused by $\bar{F}_T$, a source of heat from sediments as a result of continuously occurring seiche motions. Since actual seiche properties (period, amplitude, frequency of occurrence, etc.) have not been measured, it is difficult to know what weight should be given to the magnitude of such an estimate. However the most likely *relative* effect is to underestimate q, as follows. If a source F_T is not explicitly removed from the left-hand side of (9), it appears as an overestimate of the diffusive flux, hence of K_ν by (10). Boundary fluxes are normally considered to be proportional to the property gradient in the fluid at the boundary. With $F_T \alpha \partial T/\partial z$, K_ν from Eq. (10) is underestimated by an amount proportional to $[T(z) - T(z_b)]$, an increasing function of z (hence N); such an error results in underestimating q. (Quay *et al.* also calculated K_ν from long-term measurements of tritium injected into L224, but since this is a model-dependent determination, discussion will be deferred to the next section.)

Over the past decade, similar budget studies have been carried out in a number of sill-fjord estuaries, where the deep water (well below sill depth) provides an effectively closed system except during periods of deep water renewal. Avoiding such periods, K_ν is estimated from (10), most often using salinity S as the conserved scalar. Because it has no unknown source (sink) in the sediments, salinity is clearly preferable to temperature (heat), and the resulting K_ν determinations are probably the most accurate available to us at the present time.

Avoiding periods of deep water renewal, Svensson (1980) calculated K_ν from the budget of S within Byfjorden, a shallow-sill fjord on the west coast of Sweden. From 3 separate calculations made over time periods of 1–15 months, he reports the result $K_\nu \sim N^{-q}$ with $q \simeq 1.2$. The same relationship also resulted from the budget of rhodamine (injected into the water column at ~25 m) calculated over 3 individual periods of 1–6 months each. (Svensson argues that a low concentration of suspended

3. provided one avoids measurements taken in lakes stratified by chemical species as well as by temperature. Determination of K_ν from such systems contains two pitfalls. The first is the necessity of measuring the significant chemical concentration gradients and determining their contributions to the density gradient, hence N (for discussion, see Quay *et al.*, 1980). The second is the possibility of double-diffusive convection in systems where more than one diffusing substance determines density. In this situation, the budget method determines only an "effective" diffusivity, resulting from some unknown combination of fluxes due to internal wave breakdown and to double diffusion.

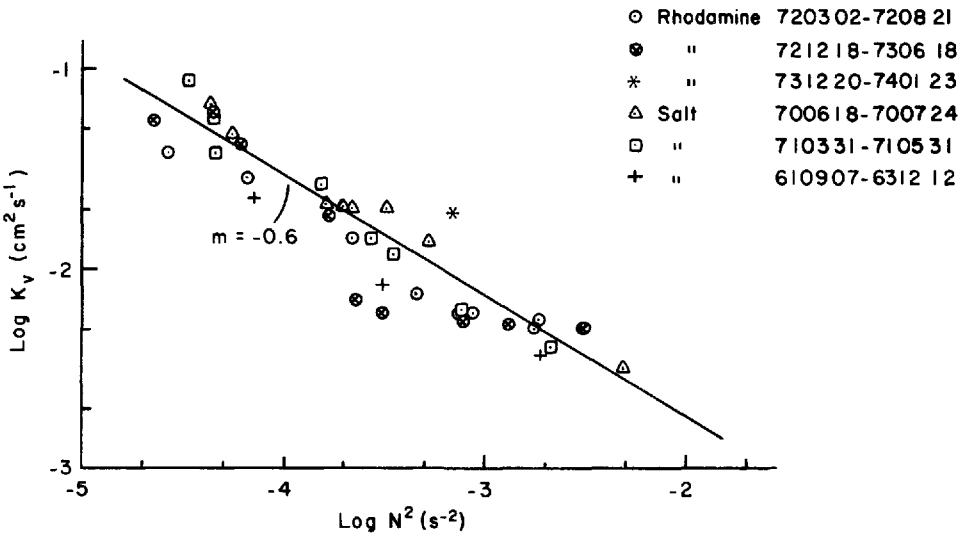

Figure 1. Vertical (diapycnal) "eddy" diffusivity K_v as a function of N^2. From Svensson (1979), who determined K_v from budgets of the conservative tracers salt and rhodamine in the deep waters of a Swedish sill-fjord (avoiding periods of advective deep water renewal): the best-fit straight line corresponds to $K_v \alpha N^{-1.2}$. Budget methods are the least model-dependent means of estimating K_v from observations (Sec. 3.1). The technique has the added advantage of determining a representative (time-averaged) value for K_v, provided it is applied over a period of time which includes many generation events for the internal waves which, in "breaking," effect the diapycnal fluxes parameterized by K_v. This time is the order of a month or more for the deep waters of sill-fjords, where the internal-wave field is predominantly generated by tidal flow.

solids and near-zero light intensity at the relevant depths makes rhodamine a conservative property in the deep waters of Byfjorden.) The combined rhodamine and salt results are shown in Figure 1. Because the measured diffusion coefficients did not correlate with variations in wind velocity or mean estuarine circulation, Svensson concluded that the energy for mixing was supplied by the tide. Smethie (1980) applied the salt budget technique to determine K_v in two Canadian west coast sill-fjords, Narrows Inlet and Princess Louisa Inlet (sill depths respectively 11 m and 6 m). In the deep waters of both inlets, where conditions for application of the budget technique are satisfied, he finds $K_v \alpha N^{-q}$ with $q \simeq 1$ for measurements over 2–3 month periods. The magnitude of K_v is 10 times greater in the bottom water of Princess Louisa Inlet than in Narrow Inlet, and Smethie points out that this is consistent with a picture of increased mixing in Princess Louisa caused by generation (and subsequent dissipation) of high frequency internal waves by tidal flow over an interior deep sill within Princess Louisa.

The most recent determination of K_v via salt budget is one carried out by the Danish Hydraulic Institute (1979) and reported by Lewis and Perkin (1982) for Agfardli-

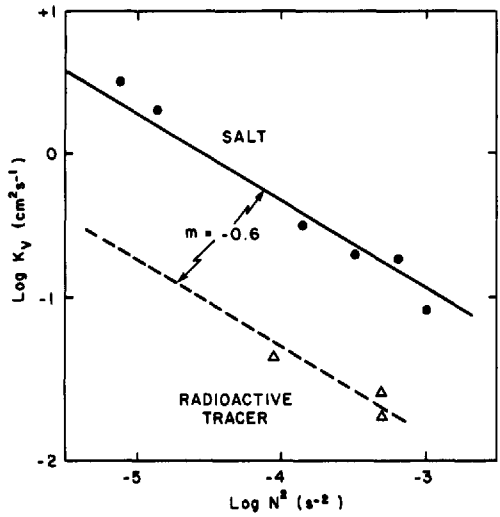

Figure 2. Determination of K_v as a function of N^2 from the salt budget for deep waters of a Greenland sill-fjord during 3 months of the stratified summer season (DHI (1979); the graph is from Lewis and Perkin (1982)): the best-fit straight line corresponds to $K_v \alpha N^{-1.2}$. Independent estimates of K_v (triangles) were also made from short-term (maximum 30 hours) measurements of the vertical spread of 'spikes' of radioactive tracer injected at different depths, hence different N. While this technique can yield accurate individual estimates of K_v (Sec. 3.2), hence (arguably) determine the functional dependence of K_v upon N, it does not yield a representative magnitude unless the measurements are repeated and time-averaged over many internal wave generation time scales (tidal periods in this case).

kavsa Fjord (A-Fjord: sill depth 20 m) on the west coast of Greenland. As shown in Figure 2, two periods of stable stratification and no deep water renewal (one of 1 month, the other of 2 months duration) gave $K_v \alpha N^{-q}$ with $q \simeq 1.2$.

The necessity for averaging over many mixing events to obtain a representative *absolute* diffusivity for a particular regime appears to be demonstrated rather clearly by further results from A-fjord. As seen in Figure 2, independent determinations of K_v from short-term (maximum of 30 hours) measurements of vertical diffusion of radioactive tracer injected at different depths (different N), gave (arguably) the same functional relationship but absolute values 10 times smaller than the salt-derived values.

Oceanic estimates of K_v by budget techniques are rare. This is partly due to the difficulty of defining closed systems, given the complex and interconnected nature of ocean basins, and partly due to measurement problems associated with the large physical extent of any such closed system, once defined. The latter problem is considerably alleviated if the scalar distribution is steady-state ($\partial c/\partial t \equiv 0$), as is the case for many deep-ocean property fields. Two recent observational studies have attempted to use this feature to determine K_v in the deep ocean from heat budget

calculations in "almost-closed" systems. For one such study, Hogg *et al.* (1982) chose the Antarctic Bottom Water (AABW, defined as water with potential temperature $\theta < 1°C$) of the Brazil Basin in the South Atlantic. Waters with $\theta < 1°C$ are supplied to the basin only through the narrow Vema Channel to the south. Hogg *et al.* divided the waters with $\theta < 1°C$ into two layers and measured the volume rate at which water was supplied to each layer through the Vema Channel. Direct estimates of volume flux from moored current meter measurements agreed with indirect estimates from geostrophic calculations relative to a reference level near 3500 m (reasons for this choice are given by Hogg *et al.*). Working up from the bottom ($\tilde{w} \equiv 0$) conservation of mass (volume) in each layer was used to estimate the area-averaged vertical velocity $\tilde{w}$ at the top of each successive layer: multiplying by the mean temperature θ of the layer yielded the vertical temperature (heat) flux which had to be balanced by a diffusive transport $K_v \partial\tilde{\theta}/\partial z$. Since the authors report that geothermal heat flux is insignificant ($F_T \equiv 0$), expression (10) for K_v reduces in this case to $K_v = \partial\tilde{\theta}/\partial z = \widetilde{w\theta}\,|_{z_1}^{z_2}$ where z_1 and z_2 are respectively the bottom and top of each layer. Hogg *et al.* calculate values of $K_v \sim 3$–$4\ \mathrm{cm^2\ s^{-1}}$, absolute values which will be re-considered in Section 3. Since N does not vary much over the limited range of the calculations, there is no observable N-dependence in these measurements.

Another application of the method described above is that of Whitehead and Worthington (1982), who attempted the steady-state heat budget for AABW (defined now as $\theta < 1.9°C$) in the North Atlantic Basin, a system supplied solely through a 300 km wide passageway between the Ceara Rise and the Mid-Atlantic Ridge near 4N. Unfortunately, their results for K_v appear much less reliable than those of Hogg *et al.*, for two reasons. The first is that they could not obtain agreement between volume transports as calculated from current meter records and from the geostrophic relation: since the input fluxes are not uniquely determined, neither are resulting values of K_v. Secondly, unlike Hogg *et al.*, they were unable to identify isotherms as isopycnals, because of small but nonzero change in θ along isopycnals over the extent of the North Atlantic Basin. In such a case, as recognized by Whitehead and Worthington, lateral mixing processes can produce cross-isotherm temperature fluxes, so that observed temperature (heat) fluxes cannot be unequivocally identified as a vertical flux.

b. Models of mean-scalar balance(s)

In this section, I consider determinations of K_v which start from Eq. (7) for the conservation of a mean scalar c (or its area-averaged counterpart $\tilde{c}$, Eq. (9)). Ideally, measurement of spatial distributions, time rates of change and source functions of *enough* (independent) scalars would determine all the unknown fields u, v, w, K_x, K_y and K_v. In reality nothing so comprehensive is possible and progress has been made only by (i) modelling Eq. (7) as a subset of its various terms, (ii) finding particular regions where fortuitous relationships between scalars eliminate some terms in a coupled-scalar equation, or (iii) assuming particular forms for some subset of the

unknown fields and solving for the rest. I will discuss these approaches separately, since each differs in philosophy, exhibits different disadvantages, and offers different information about K_v.

Method (i). The major disadvantage of method (i) is its model-dependence. When carefully applied, this method can yield useful results; however, resulting estimates for the subset of velocities and diffusivities which are retained in a particular model may reflect the assumptions which underlie the model (at least) as much as the reality inherent in the data.

As a first example, consider the technique of injecting a conservative substance c at a depth $z = z_o$ in a stratified system and measuring its spread, either horizontally to determine K_H or vertically to determine K_v. This procedure may be carried out over a short time (some hours) or a long time (many days). In the first case, it is assumed that the center of the patch is a laterally uniform environment, so horizontal mixing is (locally) unimportant and that lateral advection is unimportant provided one is following the center of the patch. The model approximation to Eq. (7)

$$\frac{\partial c}{\partial t} = K_v \frac{\partial^2 c}{\partial z^2} \tag{11}$$

which is then used to derive an estimate of K_v from measurement of the vertical spread of tracer with time (Kullenberg *et al.*, 1974; DHI, 1979) contains the implicit assumption that K_v is a constant. This assumption is valid in the context of short-period experiments, where tracer is initially (and finally) confined to a small depth range; K_v is correctly interpreted as the local value at $z \simeq z_o$ over the period of the experiment. Unfortunately, a large ensemble of such measurements would be required to determine a suitably time-averaged value for any one depth, much less determine vertical variation. This difficulty has been mentioned previously, in discussing use of this technique in A-Fjord (see Fig. 2).

Longer-period tracer experiments determine averaged values for K_v, but have other difficulties. First, long-period experiments are presently restricted to relatively small systems, where lateral boundaries restrict the horizontal spread of tracer and keep its concentration at reasonable levels for long times. This restriction would of course be eased if it proves possible to decrease detection thresholds of present tracers or new ones. A more fundamental difficulty is that, over a long-term experiment, the tracer spreads over a vertical distance which may be large enough to encompass significant variation of K_v. The type of effect which can be produced by variation of K_v is illustrated schematically in Figure 3 for a bell-shaped "initial" tracer profile with maximum at $z = z_o$. Here "initial" should be understood as that time at which the injected tracer has spread horizontally over the basin, so no lateral gradients remain in the system: consequently, the area-averaged concentration $\bar{c}$ is used in Figure 3. Such a

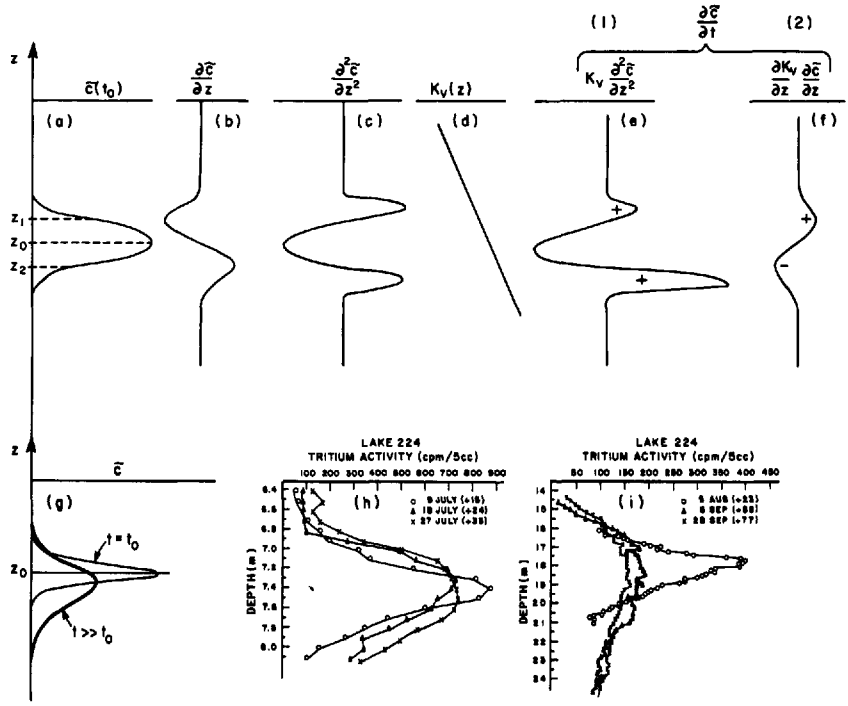

Figure 3. Schematic diagram of the effect of N-dependent K_v on results of long-term tracer injection studies. From the left, (a) the conservative tracer c (at time $t = t_o$ when horizontal uniformity has been achieved in the basin) is assumed to have a narrow bell-shaped vertical distribution about a maximum of $z = z_o$. The first (b) and second (c) derivatives of c are shown for inflection points at $z = z_1$ and z_2. (d) K_v is assumed to decrease (as N increases) upward. The last two profiles (e) and (f) represent the *two* terms which contribute to $\partial\bar{c}/\partial t$ when K_v is not constant: positive (+) or negative (−) values imply gain or loss of $\bar{c}$ with time. Term (1) dominates if the vertical scale over which K_v varies is (as drawn) much larger than the vertical scale of the initial tracer distribution, and leads to an asymmetrical vertical distribution of $\bar{c}(z, t)$ for $t > t_o$, as shown in (g). Also shown in (h) and (i) are observed profiles of tritium (^{3}H) in a stratified lake (Quay *et al.*, 1980). Vertical asymmetry, already evident in the "initial" profiles (open circles), becomes steadily more pronounced in the sense suggested here.

profile has two inflection points, denoted z_1 and z_2 in Figure 3a, so that $\partial^2\bar{c}/\partial z^2$ changes sign twice as shown. With depth-dependent K_v, the correct model equation is

$$\frac{\partial \bar{c}}{\partial t} = K_v \frac{\partial^2 \bar{c}}{\partial z^2} + \frac{\partial K_v}{\partial z}\frac{\partial \bar{c}}{\partial z}. \tag{12}$$

The second term on the right-hand side has the form of an advective change: that is, even in the absence of true advection, $\bar{c}$ may change with time due to apparent "advection" of $\partial\bar{c}/\partial z$ by a diffusive pseudo-velocity $w_d \equiv -\partial K_v/\partial z$ which arises

through vertical inhomogeneity of the diapycnal diffusion process. (Armi (1979) calls $-\nabla_H K_H$, the horizontal equivalent of w_d, a "gradient eddy diffusivity velocity": possible effects upon horizontal distributions of scalars are investigated by Armi and Haidvogel (1982). I prefer the term "diffusive pseudo-velocity" because it emphasizes that this is not a true velocity and because it lends itself to modifications, such as the double-diffusive pseudo-velocity considered in Sec. 6.)

The contributions of the two terms to observed $\partial\bar{c}/\partial t$ are shown schematically in Figure 3e and f, with positive (+) implying gain, negative (−) implying loss of $\bar{c}$ with time. The relative magnitudes have been drawn so that term (1) dominates term (2); this is the case (assumed in (a) and (d)) when the vertical scale of variation of K_v is much larger than the vertical scale of the initial tracer distribution. Upward (downward) diffusive transport is weaker (stronger) than it would be in the case of constant K_v, and over long periods, this leads to an asymmetry of the tracer distribution as shown in Figure 3g. Beside this are (h) thermocline and (i) hypolimnion (deep thermocline) tritium profiles in L224, as measured by Quay *et al.* (1980). Asymmetry is already evident in the "initial" profiles (open circles) and becomes progressively more marked as time progresses. Quay *et al.* attribute the assymmetry to "boundary conditions imposed by the lake basin" (i.e., since the area of the lake increases upward, tracer is diffusing upward (downward) into a larger (smaller) volume), and attempt to correct for this effort before determining K_v. Even when the effects of system geometry are correctly accounted for, it seems likely that long-period tracer distributions will still exhibit vertical asymmetry if K_v has significant vertical variation. Such long-period tracer measurements may be poorly represented by a model equation like (11) and would best be (re-)interpreted with the much less ambiguous budget technique discussed previously.

Method (ii). The disadvantage of a method which employs 'special' relations in order to solve for some subset of the fields involved in Eq. (7) is, of course, that the method cannot necessarily be used elsewhere to achieve the same result. Nevertheless, information on diffusivities in observationally unbounded stratified systems such as the upper ocean is so scarce that even special methods have their appeal. A useful example of such a special technique is the method of two exponential tracers, pioneered by Rooth and Ostlund (1972). For a radioactive substance c with decay constant λ, they consider an approximation to the scalar conservation Eq. (7):

$$\frac{\partial c}{\partial t} = -u_i \frac{\partial c}{\partial x_i} + K_v \frac{\partial^2 c}{\partial z^2} + \frac{\partial K_v}{\partial z}\frac{\partial c}{\partial z} + K_H \nabla_H^2 c - \lambda c. \tag{13}$$

Here ∇_H^2 is the horizontal Laplacian, the vertical diffusivity K_v and lateral diffusivity K_H ($K_x \sim K_y \sim K_H$) are considered to be functions of vertical coordinate only and there are no *in-situ* sources or sinks of c other than radioactive decay. Assuming that the

diffusion coefficients for c and for temperature T are identical, the steady-state heat equation may be written

$$0 = -u_i \frac{\partial T}{\partial x_i} + K_v \frac{\partial^2 T}{\partial z^2} + \frac{\partial K_v}{\partial z}\frac{\partial T}{\partial z} + K_H \nabla_H^2 T. \tag{14}$$

Rooth and Ostlund noticed that if there exists some depth range within which both c and $T - T_o$ (for some constant T_o) have exponential distributions with depth, characterized by scale depths H_c and H_T respectively, then it is possible to write a coupled equation from which the advective terms have cancelled exactly. First note that if

$$(T - T_o) = T' \exp\left(\frac{z}{H_T}\right) \text{and } c = c'(t) \exp\left(\frac{z}{H_c}\right), \tag{15}$$

then $\ln c = \phi_o(t) + \mu \ln (T - T_o)$, where $\mu = H_T/H_c$ and $\phi_o(t) = [\ln c' - \mu \ln T']$. Defining $\ln c = \phi$ and $\ln (T - T_o) = \theta$, (15) may be rewritten as $\phi = \phi_o + \mu\theta$ and used to couple Eqs. (13) and (14), with the result

$$\phi_t + \lambda = (\mu^2 - \mu)\left[K_v\left(\frac{\partial \theta}{\partial z}\right)^2 + K_H(\nabla_H \theta)^2\right],$$

Since $|\partial\theta/\partial z|^{-1} \sim H_T$ and $|\nabla_H \theta|^{-1} \sim L_T$ are characteristic vertical and horizontal scale lengths of the thermocline, the above equation can finally be written as (Eq. (7) of Rooth and Ostlund):

$$\phi_t + \lambda = (\mu^2 - \mu)\left[\frac{K_v}{H_T^2} + \frac{K_H}{L_T^2}\right]. \tag{16}$$

The local rate of change θ_t, adjusted by the decay rate λ, is balanced by an effective diffusion rate *regardless* of advective effects and boundary conditions. Rooth and Ostlund applied Eq. (16) to observations of tritium and temperature in a part of the water column just below the Eighteen Degree Water in the Sargasso Sea, where values of $\lambda = (12.26 \text{ yr})^{-1}$, $\mu = 5$ and $H_T = 440$ m were known quite precisely. They were forced to estimate θ_t more approximately, but concluded that it should result in at most a 30% increase in the estimated diffusion term: thus, introducing an "effective diffusivity" K_e which includes both horizontal and vertical effects,

$$K_e \equiv \left[K_v + \frac{H_T^2}{L_T^2} K_H\right] < 0.23 \text{ cm}^2 \text{ s}^{-1}.$$

Since $(H_T^2/L_T^2)\, K_H > 0$, this relation provides only an *upper bound* on K_v; interpreting K_e in terms of the dominance of either vertical or lateral mixing requires further information.

This inability to separate the effects of vertical and lateral diffusion recurs in tracer studies. A recent example is the work of Gammon *et al.* (1982), describing measured vertical distributions of the halomethanes F11 (CCl_3F) and F12 (CCl_2F_2) in the

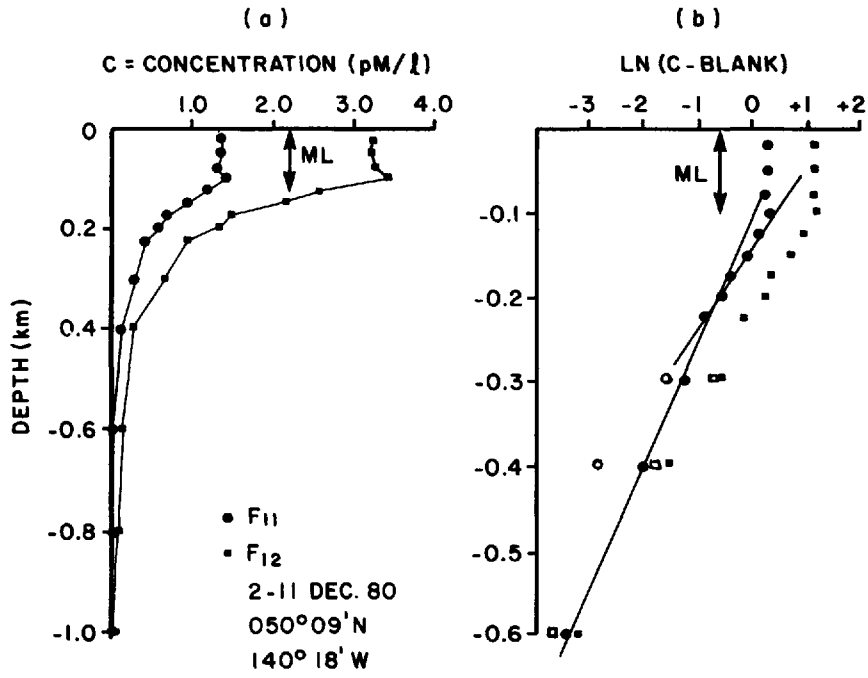

Figure 4. (a) Concentrations of the halomethanes Freon 11 (F11) and Freon 12 (F12) as functions of depth, as observed by Gammon *et al.* (1982) in the subarctic gyre of the northeast Pacific. Values are averages over 5 profiles taken within a one-week period. (b) The logarithm of concentration, corrected for a system blank level, plotted as a function of depth. Straight-line segments in such a plot reveal parts of the water column in which the tracer concentration behaves as a logarithmic function of depth: the slope of the lines shown are proportional to H_c, where H_c is a tracer scale depth. Coupling H_c to the exponential scale depth H_T of the (steady-state) thermocline yields an upper bound on K_v, by a method originally due to Rooth and Ostlund (1972).

subarctic gyre of the eastern North Pacific. A sample of the observational data is shown in Figure 4; values are averages of 5 casts at 50°09'N, 140°18'W over a one-week period. The model equation chosen by Gammon *et al.* (their Eq. (1)) is considerably simpler than Eq. (13) because they have made the additional assumptions that horizontal gradients are negligible and that both K_v and w are constants. However the governing equation need not be this simple: since the system is eventually closed by using the exponential nature of the vertical distributions of tracer and of temperature, the assumptions may be eased to those of Rooth and Ostlund and a solution sought in a similar way. The only difference is that the halomethane concentration in the stratified interior of the upper ocean is driven by a source function at the base of the mixed layer

$$c(z_m,t) = c_o \exp\left(\frac{t}{\tau}\right)$$

where $c(z_m,t)$ is the mixed layer concentration, assumed to track an atmospheric source function which grows exponentially with characteristic time $\tau = 6.7$ yr. for F11 (9.6 yr. for F12). The vertical distribution of c over a depth range of 200–600 m is found to be exponential with scale depth $H_c \simeq 122$ m for F11 (143 m for F12) while the scale depth for the thermocline over this range is $H_T \simeq 300$ m. Thus $\mu \equiv H_T/H_c = 2.5$ for F11 (2.1 for F12). With $\lambda = 0$ and $\phi_t \equiv c_t/c = \tau^{-1}$, as expected for $t \lesssim 3\tau$ (see Gammon *et al.*, 1982), Eq. (16) yields

$$K_v \leq K_e \equiv \left[K_v + \frac{H_T^2}{L_T^2} K_H \right] = \frac{H_c^2}{\tau} \frac{\mu}{\mu - 1} \simeq 1.2 \text{ cm}^2 \text{ s}^{-1} \tag{17}$$

for both freons. This result is *independent* of any advective field, but suffers the usual indeterminancy with respect to vertical/lateral mixing. Gammon *et al.* feel that it is very doubtful that the effective diffusivity could result largely from lateral rather than vertical effects, but this seems far from proven. Comparing F11 concentrations at 50N with values reported from a near-coastal environment at 46N *along isopycnals* (density values kindly supplied by R. Gammon) reveals isopycnal gradients of order $\text{F11}/\Delta Y = \sim 1 \times 10^{-8}$ pmol/l/cm. In such a case, where isopycnal gradients of tracer demonstrably exist but are not well mapped, it is not easy to prove that observed tracer distributions must be produced by local vertical processes rather than by lateral processes distributing effects of laterally inhomogeneous vertical processes. This point is made by the authors but bears repetition: a parametric model, such as that obtained by interpreting the effective diffusivity $K_e \simeq 1.2$ cm^2 s^{-1} as that due to vertical processes alone, may "work" well, in the sense of having useful predictive ability, without resolving fundamental questions about the physical behavior of the system.

Figure 4b contains a suggestion of depth-dependence of the effective diffusivity K_e, in the fact that the upper depth range of 100–200 m is characterized by a slope $(H_c)_u$ which is smaller than the slope H_c reported by Gammon *et al.* for the deeper range of ~200–600 m. Rough fits in Figure 4b suggest that $(H_c)_u \simeq H_c/2$ (hence $(\mu)_u \simeq 2\mu$): from (17), using an average value of $\mu \sim 2.3$

$$(K_e)_u = \frac{1}{4}\left(\frac{\mu - 1}{\mu - 0.5} \right) K_e \simeq 0.2\, K_e \sim 0.2 \text{ cm}^2 \text{ s}^{-1} .$$

Such an increase in K_e with depth would be consistent with an inverse dependence of K_v on N (among other possibilities). Unfortunately, as mentioned by Gammon *et al.*, any such conclusion is rather sensitive to the assumed blank (measurement noise) level subtracted from the data before plotting as Figure 4b. Using F11 as an example, if instead of taking the lowest observed value at 800 m (0.02 pmol/l) as the blank, one were to use the average of all 8 values at 800 m (0.10 pmol/l), the solid symbols in Figure 4b would be replaced by the open symbols. The largest differences are of course

in the deepest values since these are closest to the system blank level (the mean value at 600 m was *less* than 0.10 pmol/l, hence is not plotted), and are very nearly sufficient to transform the slope of the deep region to that of the upper. Thus the halomethane data appear insufficient to reveal any N-dependence of K_v. It does suggest an upper bound of order 0.2 $cm^2\ s^{-1}$ for K_v in the depth range of ~100–200 m in the northeast Pacific.

Method (iii). The final method of estimating K_v consists of assuming that the underlying circulation (i.e., $\mathbf{u}$) is known, and then choosing K_v and K_H ($\simeq K_x \simeq K_y$) in order to "best fit" observed distributions of various scalars (a process usually accomplished numerically). To date, the scalar fields used have inevitably been those of steady-state tracers ($\partial c/\partial t = 0$), in view of an otherwise difficult observational problem. A major disadvantage to this method is obvious: if the underlying circulation is incorrect, the resulting values (more usually bounds) for K_v and K_H are also incorrect.

The technique is most surely applied if there is reason to believe that $\mathbf{u} \equiv 0$, i.e., that there is no net (time-averaged) circulation, as is likely the case in closed basins of small enough size. As an example, consider the Santa Barbara Basin, in which Lietzke and Lerman (1975) examined spread of the scalar ^{222}Rn, a short-lived ($\lambda = (3.8\ da)^{-1}$) radioactive isotope with a source in the sediments. Since the dimensions of the basin (~ 20 × 30 km below sill depth of 475 m) are not significantly larger than an internal Rossby radius of ~20 km (roughly calculated using an average water depth of 575 m and assuming a value of $N \simeq 3$ cph), the basin is not expected to contain a mean circulation. Setting $\mathbf{u} \equiv 0$, assuming K_v and K_H to be constant, and applying the observed bottom source of ^{222}Rn, Lietzke and Lerman numerically solved Eq. (7) for various values of K_v and K_H. As might be expected, the results show that when vertical diffusion is chosen to dominate lateral diffusion, ^{222}Rn-isolines parallel the bottom relief. When lateral diffusion dominates, its effects counteract decay and bring ^{222}Rn to the center of the basin, resulting in nearly horizontal isolines. In this study, the (rather scant) observational evidence available favored the first case: the best fit suggested that vertical diffusion ($K_v \simeq 4\ cm^2\ s^{-1}$) dominated lateral diffusion ($K_H \sim 10^6\ cm^2\ s^{-1}$). Smethie (1980) reports a similar result, i.e., ^{222}Rn-isolines tending to parallel bottom topography, from more extensive transects in Dabob Bay, an inlet off Puget Sound which is also expected to have nearly zero net circulation.

On the larger scale of ocean basins, some nonzero advective field must be assumed. Since upper ocean circulation, subject to near-field effects of variable wind and buoyancy forcing, is not imagined to be in a steady state, basin-scale applications of method (iii) are generally confined to the "abyssal" ocean (i.e., below the thermocline) and the circulation is usually assumed to be some variation of that due to Stommel (1958) and Stommel and Arons (1960a and 1960b). The abyssal ocean is assumed to

be homogeneous with density ρ_o and to extend from a flat bottom at $z = 0$ to the base of the thermocline at $z = H$. In the interior of ocean basins, the flow is assumed to be

geostrophic
$$-fu = \frac{1}{\rho_o}\frac{\partial p}{\partial y} \tag{18}$$

$$fv = \frac{1}{\rho_o}\frac{\partial p}{\partial x} \tag{19}$$

hydrostatic
$$g\rho_o = -\frac{\partial p}{\partial z} \tag{20}$$

and incompressible
$$\frac{\partial u}{\partial x} + \frac{\partial v}{\partial y} + \frac{\partial w}{\partial z} = 0 \tag{21}$$

(the equations governing the flow are written in rectangular coordinates for simplicity: however the general results also follow when the system is examined in the spherical coordinates more appropriate for basin-scale flows). The associated vorticity equation, derived by cross-differentiating Eqs. (18) and (19) and using (21), is given by

$$v = \frac{f}{\beta}\frac{\partial w}{\partial z}. \tag{22}$$

Such a flow is barotropic; i.e., $\partial u/\partial z = \partial v/\partial z = 0$ and the associated vertical velocity field, constrained by $\partial^2 w/\partial z^2 = 0$ (from 22)), is a *linear function of z,*

$$w = w_o + (w_H - w_o)\frac{z}{H}. \tag{23}$$

Here w_o is the vertical velocity at the bottom boundary $z = 0$ (this may be thought of as the solid boundary, in which case $w_o = 0$, or perhaps as the top of some frictionally-dominated bottom boundary layer which supplies fluid to the geostrophic interior; in this case $w_o > 0$) and w_H is the vertical velocity at the base of the thermocline. Under these constraints, the two possible choices for $w(z)$ are shown in Figure 5. Stommel (1958) originally chose $0 \leq w_o < w_H$, requiring $w_H > 0$ for consistency with a diffusive model of the main thermocline of subtropical gyres (Robinson and Stommel, 1959): the same choice was made by Stommel and Arons (1960), Kuo and Veronis (1973), and Fiadeiro and Craig (1978; model (a)). The choice of $w_H < 0 \leq w_o$ (Fig. 5b) is considered more reasonable for subpolar gyres: Wyrtki (1961) and Fiadeiro and Craig (1978; model (b)) allow for this by setting $w_H \alpha \cos 3\theta$. In all of these models, the *direction* of the meridional component v of the flow in the geostrophic interior is completely determined by the sign of $\partial w/\partial z$; i.e., by whether w_H is greater or smaller than w_o (Eq. (22)). In both hemispheres, if $\partial w/\partial z > 0$ (Fig. 5a), v is poleward: if $\partial w/\partial z < 0$ (Fig. 5b), v is equatorward. Once $w_H = w_h f(\theta)$ (hence the direction(s) of the interior meridional circulation) is fixed, the directions of flow in ageostrophic western and/or northern boundary currents are fixed by mass conservation, given the

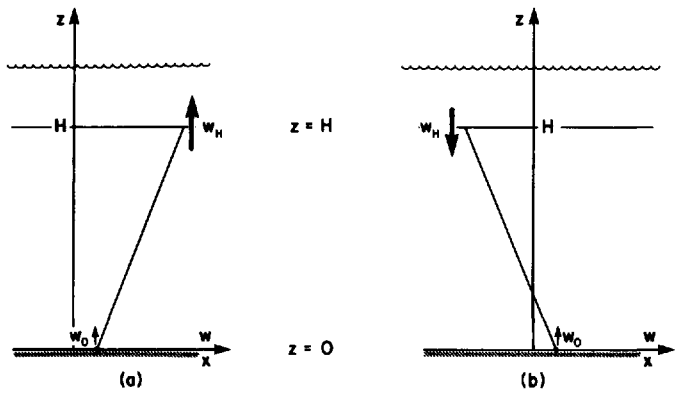

Figure 5. If the interior flow of the deep ocean (below the main thermocline) is assumed to be geostrophic, hydrostatic and incompressible, the associated vertical velocity field is a linear function of z. In this schematic, w_o is the vertical velocity at $z = 0$ (this may be thought of as a solid boundary ($w_o = 0$), or perhaps as the top of a bottom boundary layer which supplies fluid ($w_o > 0$) to the geostrophic interior) and w_H is the vertical velocity at $z = H$, the base of the thermocline. (a) The choice $0 \leq w_o < w_H$; ($\partial w/\partial z > 0$) made by Stommel (1958) implies poleward meridional flow. (b) The choice $w_H < w_o$; ($\partial w/\partial z < 0$) implies equatorward interior flow.

location(s) of source regions where bottom water is assumed to form. In this regard, most models follow Stommel (1958) in locating sources at high latitudes in the North Atlantic and in the Weddell Sea. The *magnitudes* of the interior circulation and boundary fluxes can be related to the basin-integrated value of the upwelling flux at $z = H$ (Stommel and Arons, 1960b). Thus the unknown magnitude of the circulation can be characterized by the single parameter w_H (or w_h) which, if known, closes the mass transport. Models of conservative scalar distributions, however, require introduction of a further unknown circulation parameter R, technically the recirculating transport of the Antarctic Circumpolar Current, which forms an open southern boundary to all the major ocean basins. The parameter R must be chosen to simulate effects of diffusion of scalars across the open southern boundary of the real basin in computations which of necessity impose a closed southern boundary condition (for further discussion, see Fiadeiro and Craig, 1978).

Once the circulation has been parameterized, there remains the problem that while many standard oceanographic variables are dynamically passive, few are conservative. Addition of an observed nonconservative scalar field does not further constrain circulation parameters and diffusivities because a poorly known *in-situ* source/sink function is added to the list of unknowns. As an example, Fiadeiro and Craig (1978) modelled distributions of the conservative scalar salinity S and the nonconservative tracer oxygen O_2 in the Pacific. They were forced to assume a form for w_H: to be consistent with Stommel (1958), Munk (1966) and Craig (1969), they chose a uniform

upwelling velocity of $w_H = 3\text{m y}^{-1}$ ($\sim 1 \times 10^{-5}$ cm s^{-1}). Then $R = 10^7$ m^3 s^{-1} = 10 Sv was determined by requiring that the S distribution vary smoothly between observed vertical distributions at the east and west ends of the southern (ACC) boundary: R had only a slight effect on the interior solutions, so its value was not critical. Finally, diffusivities were determined by comparing observed horizontal and vertical S sections with model solutions (forced by the horizontal S distribution observed at 1 km) employing a variety of K_v and K_H. The solutions deemed acceptable provided acceptable ranges for the diffusivities

$$0.5 \text{ cm}^2 \text{ s}^{-1} < K_v < 1.0 \text{ cm}^2 \text{ s}^{-1} \text{ and } 10^6 \text{ cm}^2 \text{ s}^{-1} < K_H < 10^7 \text{ cm}^2 \text{ s}^{-1}:$$

the "best" fit used $K_v = 0.6$ cm^2 s^{-1} and $K_H = 5 \times 10^6$ cm^2 s^{-1}. Addition of the O_2 distribution merely served to determine a (parametric) form for the O_2 source function due to in-situ regeneration.

An additional *conservative* tracer can of course be used to further constrain system parameters. To the S distribution in the Pacific, Fiadeiro (1982) added the observed distribution of the (nearly) radioconservative tracer ΔC^{14}, the C–14/C–12 ratio. He found that while the salinity distribution could be reasonably described by a model of the type described above, such a model was totally unable to reproduce the pronounced mid-depth ΔC^{14} minimum observed over extensive regions of the northeastern Pacific. At this point one may attempt to improve the model fit for ΔC^{14} (without of course degrading the fit for S) by modifying *either* the circulation or the diffusivities: which one chooses is primarily a matter of taste. Fiadeiro chose to modify the circulation, postulating a sign reversal of $\partial w/\partial z$ at some height z_o above the bottom. Choosing $z_o = 1$ km above the bottom in an ocean of depth 4 km as an approximate boundary between "deep" and bottom waters in the South Pacific, Fiadeiro explored model sensitivity to four parameters w_{z_o}, w_H, K_v and K_H. He found best fits for both S and ΔC^{14} with $w_{z_o} = 2.6\text{ m y}^{-1}$ (0.8×10^{-5} cm s^{-1}), $w_H = 1.0\text{ m y}^{-1}$ (0.3×10^{-5} cm s^{-1}), $K_v = 0.6$ cm^2 s^{-1} and $K_H = 5 \times 10^6$ cm^2 s^{-1}. The fields of S and ΔC^{14} are affected quite differently by the various parameters: certain features show opposite tendencies with respect to the ratio of advection to vertical diffusion, while the effect of varying K_H is substantial in the ΔC^{14} solution and relatively minor in the S solution. Consequently, the resulting values of K_v and K_H are much more tightly constrained than those obtained by Fiadeiro and Craig: they are nevertheless *still constrained to be constant.* In this sense the value obtained for K_v (and K_H) is still crucially model-dependent.

c. Models of scalar variance

To date, all observations of scalar variances have been interpreted with the model of Osborn and Cox (1972) originally developed for application to the scalar temperature T by starting from an entropy equation. For a generalized scalar c, the Osborn–Cox model is equivalent to starting with the assumptions inherent to Eq. (8), then further assuming that (i) the scalar fluctuation variance is both steady-state and spatially

nondivergent under suitable ensemble averaging (denoted by an overbar) and (ii) the mean scalar field is laterally homogeneous in the sense that $K_e \equiv [K_v + (H_T^2/L_T^2) K_H] \simeq K_v$ (in the notation of the previous section). Then Eq. (8) reduces to

$$K_v \left(\frac{\partial c}{\partial z}\right)^2 = \frac{\chi_c}{2} = D_c \overline{\left(\frac{\partial c'}{\partial x_i}\right)^2} \tag{24}$$

and the vertical eddy diffusivity can be expressed as $K_v = D_c C_3$, the product of molecular diffusivity D_c and a parameter

$$C_3 \equiv \frac{\overline{\left(\frac{\partial c'}{\partial x_i}\right)^2}}{\left(\frac{\partial c}{\partial z}\right)^2}.$$

When the scalar $c = T$, C_3 is known as the three-dimensional Cox number, and is the ratio of two measurable (theoretically at least) quantities, the mean vertical temperature gradient $\partial T/\partial z$ and the full 3-dimensional variance of scalar gradient fluctuation (dominated by the smallest microstructure scales of the temperature field). What is in fact presently measurable is *one* of the three components of the gradient variance, most often the vertical component $\overline{(\partial T'/\partial z)^2}$ from vertical profilers (Osborn and Cox, 1972; Gregg, 1977, 1980; Oakey and Elliott, 1977; Caldwell *et al.*, 1980; to name but a few) but occasionally one horizontal component from a towed system (Gargett, 1976; Washburn and Gibson, 1982). If the smallest scales of the temperature fluctuations are isotropic, then $\overline{(\nabla T')^2} = \overline{3(\partial T'/\partial z)^2}$: if they are completely anisotropic, one expects $\overline{(\nabla T')^2} = \overline{\partial T'/\partial z)^2}$ for a stratified fluid. Thus $K_v = D_T(1\text{–}3)\ Cx$, where Cx is a one-dimensional Cox number. There has been considerable discussion in the literature about the degree of isotropy (hence the choice of the factor 1–3), of temperature microscales (Gregg, 1977, 1980; Gibson, 1980; Caldwell *et al.*, 1980). Gregg (1977, 1980) routinely chooses 1, arguing that comparison of vertical and quasi-horizontal temperature measurements shows little evidence of isotropy down to scales of 10 cm. My own bias is toward 3, for the following reasons. First: measurements of all three components of the turbulent *velocity* field in a highly stratified estuarine system show that the velocity field approaches isotropy by the peak of its dissipation spectrum for values of kinetic energy dissipation rate comparable to those typically observed in the ocean, when scaled for the large difference in N (Gargett *et al.*, 1984). If the velocity field achieves isotropy by *its* dissipation scales, there seems little excuse for the temperature field not to reach isotropy by the temperature dissipation scales, which occur at considerably higher wavenumbers. Indeed, both Dillon and Caldwell (1980) and Oakey (1982) have observed universal high-wavenumber shapes for fully resolved temperature gradient spectra. Second: the ensemble averages involved in Eq. (24) are

dominated by the records with the largest Cox numbers, and these are records for which the available evidence does indicate an approach to isotropy. For example, Gregg (1977) presents evidence for full stratification in a record with $Cx = 1$ but significant departures (which one may interpret as an approach to isotropy) in a record with $Cx = 12$ (the system response apparently limits this record to wavenumbers less than 1.7 cm, but the deviation from full stratification presumably continues to the higher wavenumbers of the remainder of the temperature dissipation spectrum).

Although a growing body of microscale temperature observations exists, the only repeated determinations of K_ν in a single area are the vertical profiler results of Gregg (1977, 1980) near 28N, 155W in the North Pacific. Figure 6 reproduces data (from Fig. 8 of Gregg (1977)) taken during three cruises to this site. The triangles added to this plot are ensemble means, over all three cruises, of Cx for realizations between 0.2–0.6 km and 0.8–1.2 km respectively. Before estimating K_ν, measured values of Cx must be corrected for poorly known thermistor response. Gregg (1976) found that the variance of mixed layer records which followed a universal Batchelor (1959) shape over the measured wavenumber range was a factor of 2 less than that obtained from integration of the full Batchelor spectrum. Gregg (1977) suggested that this factor of 2 should be considered an upper bound to the correction necessary for the weaker turbulence in the stratified ocean. However, reiterating the above argument that ensemble averages are dominated by the highest Cx records; i.e., those most severely underestimated by probe roll-off, I shall choose the full factor of 2. Finally, then

$$K_\nu = D(3)\,(2)Cx = 6D\,Cx$$

(note that Gregg (1977) considered that the most likely underestimate was a factor of 4). Using this expression with the upper (0.2–0.6 km) and lower 0.8–1.2 km) ensemble averages of $Cx = 7$ and 59 respectively, gives estimated values of $K_\nu = 0.06$ and 0.49 $cm^2\,s^{-1}$ which increase with increasing depth (decreasing N).

Unfortunately, these results (and others obtained with the Osborn-Cox model) are once again only upper bounds on K_ν, as a result of two model assumptions. The first, mentioned previously, is the assumption that $K_e \simeq K_\nu$; i.e., that vertical mixing is dominant. The second is the assumption that an appropriate ensemble-average of scalar fluctuation variance is spatially nondivergent; i.e., that terms such as $\partial/\partial x_i \overline{(u_i'\,(c')^2)}$ are negligible. This assumption is increasingly being questioned. Armi (1979) argues that lateral divergences may dominate the scalar variance balance, while Holloway (1983) (see also GH) conjectures that observed shapes of kinetic and potential energy spectra can be explained by assuming dominance of the vertical divergence term. With either of these balances, estimates of K_ν based upon Cox number will be overestimates, hence upper bounds on the true values.

4. A suggested form of oceanic K_ν due to internal wave "breaking"

The preceding examination of observational evidence regarding K_ν in stratified geophysical systems assumed to be mixed mainly by internal wave "breaking" has

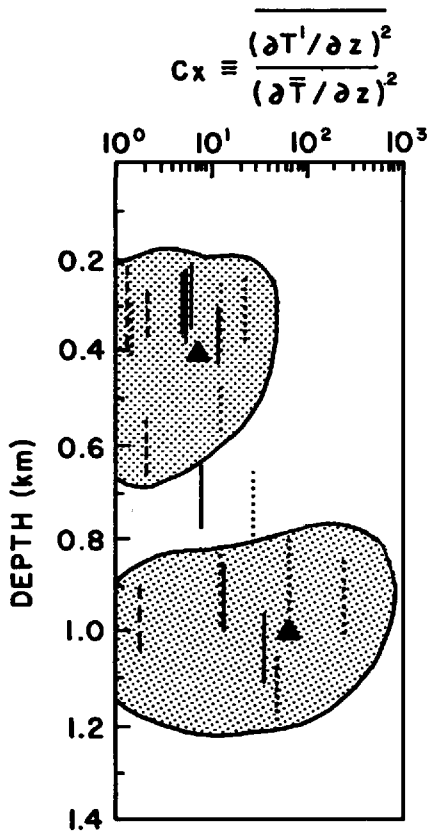

Figure 6. Measurements of the one-dimensional Cox number Cx as a function of depth near 28N. 155W in the northeastern Pacific subtropical gyre (after Fig. 8 of Gregg (1977)). Triangles represent averages over all values in the depth ranges 0.2–0.6 km ($\overline{Cx} = 7$) and 0.8–1.2 km ($\overline{Cx} = 59$). Averaged values of Cx can be transformed to an estimate of K_v using the model of Osborn and Cox (1972): assumptions inherent in this model imply that the resulting value is only an upper bound on K_v.

attempted to determine which estimation techniques are most trustworthy; i.e., least model-dependent. Of the three techniques discussed, the only unequivocal results come from the budget method for conservative tracers, applied to closed basins in which the tracer is laterally well-mixed. Various applications of this technique suggest an inverse dependence of K_v on N of the form $K_v \alpha N^{-q}$ with $q \sim 0(1)$, the upper limit (Case 1) of the range suggested by GH (Section 2).

In order to discuss possible oceanic consequences of an N-dependent K_v, I would like to estimate not only a functional dependence, but an amplitude: i.e., determine the "constant" a_o in the relation

$$K_v = a_o N^{-1} \tag{25}$$

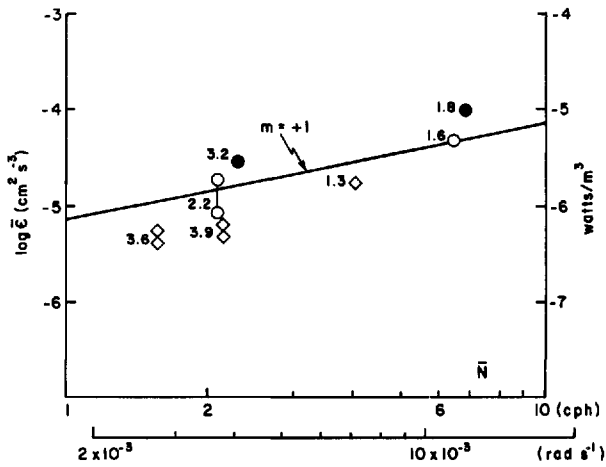

Figure 7. Individual values of kinetic energy dissipation rate ϵ over $\Delta z \simeq 2$ m can be determined by airfoil probe measurements of two components of the dissipation tensor (Osborn and Crawford, 1980) by invoking dissipation-scale isotropy (Gargett *et al.*, 1984). This plot presents available cruise-averaged values of $\bar{\epsilon}$ and $\overline{N}$. The number beside each symbol indicates the number of kilometers sampled and the spread between joined symbols is an effect of measurement noise. The circles are observations taken in the Sargasso area of the western North Atlantic subtropical gyre, both far from boundaries (open circles) and close to the island of Bermuda (closed circles): Gargett and Osborn (1981). Triangles are observations of Lueck *et al.* (1983) in the eastern boundary region of the North Pacific subarctic gyre; observations in this area, while still confined to the upper kilometer in depth, reach a lower value of N. The relationship $\bar{\epsilon} = (4 \times 10^{-3}\ \mathrm{cm^2\ s^{-2}})\ \overline{N}^{+1}$ (straight line) approximates the data within a factor of 2–3, roughly the degree of universality expected if $\bar{\epsilon}$ arises through processes associated with a "universal" deep ocean internal wave field.

for the oceanic system. Following the reasoning of GH, the constancy of a_o should be of the same degree as the universality of an (appropriately time-averaged) internal wave field which supplies energy to the scales which accomplish diapycnal mixing. The actual value of a_o will depend upon individual systems, since it is dependent upon the rate at which energy is being passed through the internal waves to small scales (proportional to the rate at which a steady-state internal wave field is forced). Thus, unlike values of q, values for a_o determined from lakes and estuaries will *not* be applicable to the oceanic internal wave field. I have chosen to estimate a_o from Eq. (2), using the averaged estimates of oceanic $\bar{\epsilon}$ shown in Figure 7. The relation $\bar{\epsilon} = (4 \times 10^{-3}\ \mathrm{cm^2\ s^{-2}})\ \overline{N}^{+1}$ is plotted: this choice approximates the data within a factor of 2–3, about the same degree of universality claimed for observations of the oceanic internal wave field (Garrett and Munk, 1972). Using a value of $R_f \simeq 0.20$ (see GH for available evidence regarding this choice), the resulting value for $a_o = 1 \times 10^{-3}\ \mathrm{cm^2\ s^{-2}}$.

Figure 8 shows typical vertical profiles of $N(z)$ from two locations in the North Pacific (a) subarctic gyre near 50N, 145W and (b) subtropical gyre near 28N, 155W: estimates from two bottle casts at each station have been smoothed by eye. Also plotted

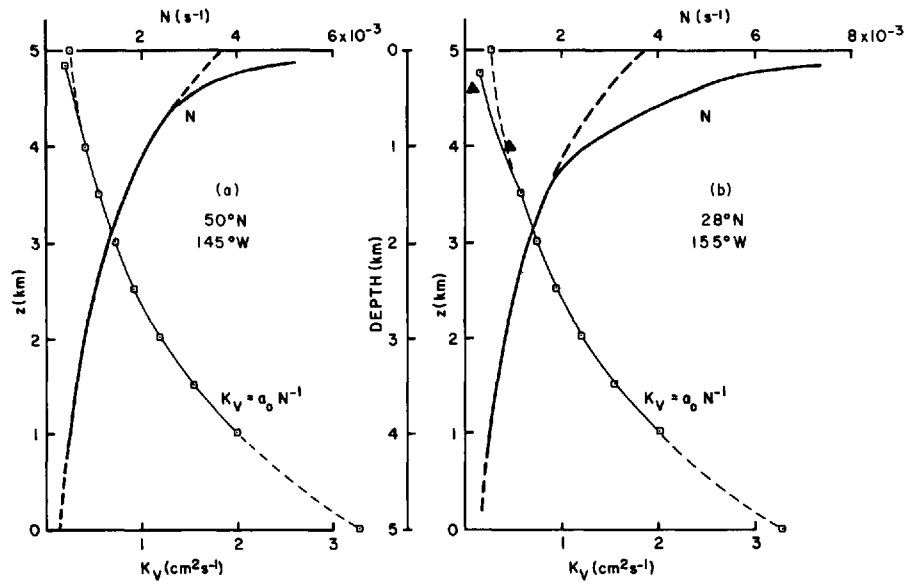

Figure 8. Buoyancy frequency N as a function of depth (middle scale) or of height z above 5 km depth, at locations within the (a) subarctic and (b) subtropical gyres of the North Pacific (estimates from two bottle casts at each location were smoothed by eye). For depths below ~1 km, both N profiles are reasonably approximated by the exponential function $N(z) = N_o \exp((z - B)/2b)$: $b = 1$ km is a scale depth for the deep pycnocline and N_o is an "abyssal" value for N, here chosen as $N_o = 5 \times 10^{-4}$ s^{-1} (0.28 cph) at $z = B = 1$ km (near the average bottom depth of 4 km). This exponential has been extrapolated to higher and lower stabilities (heavy dashed curves) for illustration only: it underestimates N in the upper part of the water column, most seriously in the subtropical gyre. Light lines in both panels are profiles of $K_v = a_o N^{-1}$, using $a_o \simeq 1 \times 10^{-3}$ cm^2 s^{-2} and either actual (solid lines) or extrapolated (dashed lines) values of N. Triangles superimposed on (b) are upper bound estimates of K_v from microstructure measurements at this location (Gregg, 1977).

are corresponding values of K_v, calculated from (25) with the above value of a_o determined from measurements of $\bar{\epsilon}$. The triangles in Figure 8b are the average upper bound values of K_v derived from Gregg's temperature microstructure measurements at the same location. The agreement with the predicted values is remarkable.[4] Predicted values of K_v are small in the upper kilometer of the ocean (particularly of the more highly stratified subtropical gyres), consistent with available upper bound estimates of $0(0.1$ cm^2 s$^{-1})$. A value of $K_v \sim 1$ cm^2 s^{-1} is reached at a depth of ~2.5 km, while

4. Although possibly fortuitious. As suggested by Gibson (1981), it is not yet clear how much microscale data are enough for a meaningful average. I have assumed that the values of $\bar{\epsilon}$ in Figure 7 are "sufficiently" averaged, because cruise-averaged values from different oceans and different depth ranges (although comparable ranges of N) do not differ by more than a factor of 2 or 3. The temperature microstructure data involve somewhat smaller sample values (~1.6 km and 1.2 km for upper and lower ranges respectively) hence are more subject to underestimation due to under-sampling. Such an underestimate could compensate for all or part of an overestimate due to the problems discussed in connection with method (iii).

predicted values in the depth range of 4–5 km are ~2–3 $cm^2\ s^{-1}$, in rough agreement with the estimates of Hogg *et al.* (1982).

5. Oceanic implications of an N-dependent K_v

The inclusion of vertical variation of K_v, through its dependence upon N, produces some novel features within the context of older models which attempted (in the simplest possible way, since available data were both limited and in some cases inaccurate) to account for the steady-state nature of the large-scale density field in the deep ocean, despite evidence of continuing formation of deep and bottom waters.

As an example, let us suppose that in the stratified interior of ocean basins, far from western boundary regions and *below* the main pycnocline, the density field is maintained by a balance between upward advection and downward turbulent diffusion (for the scaling arguments which suggest such a balance, see Warren, 1977). Consider an ocean basin in which bottom water is supplied in horizontally limited regions at high latitudes, becomes distributed laterally (by unidentified processes) throughout the basin in a bottom boundary layer which occupies some fraction of the bottom kilometer, then upwells across isopycnals throughout the basin. The density equation expressing a local balance between vertical advection and diffusion is given by:

$$w\rho_z - (K_v \rho_z)_z = 0. \tag{26}$$

If w and K_v are independent of depth, Eq. (26) reduces to

$$w\rho_z - K_v \rho_{zz} = 0, \tag{27}$$

the simplified vertical advection/diffusion model of Munk (1966). Eq. (27) has the property that

$$\frac{w}{K_v} = \frac{\rho_{zz}}{\rho_z} = \frac{1}{b} \tag{28}$$

if the time-mean density distribution has the functional form

$$\rho(z) = \rho_o - \Delta\rho \exp((z - B)/b) \tag{29}$$

i.e., an exponential function of scale depth b and density $(\rho_o - \Delta\rho)$ at $z = b = 1$ km. (Values of b in the range 0.7–1.1 km produce a reasonable first-order description of many deep ocean density profiles (Chung, 1975): I have used $b = 1$ km in Fig. 8.) The magnitude of w_B, the upwelling speed at the top of the bottom boundary layer (hence also the upwelling speed at the base of the pycnocline in this z-independent model) has been estimated by various methods. Munk (1966) used vertical profiles of tracers such as ^{226}Ra and ^{14}C to estimate $w_B \sim 1.4 \times 10^{-5}$ cm s^{-1}, a value consistent with his order-of-magnitude estimate of the rate of formation of Antarctic Bottom Water. From evidence of high-latitude deep and bottom water formation in the North Atlantic

(Worthington, 1969) and Antarctic (Carmack and Foster, 1975), it is clear that vertical return flow *must* take place, and that the necessity of a vertical upwelling velocity w_B of order 1×10^{-5} cm s^{-1} can be escaped only by requiring much larger vertical velocities in geographically restricted areas. Although this latter possibility cannot be dismissed utterly, it is unlikely that its effects on deep-water property distributions would have gone un-noticed (Warren, 1981). Thus we are left with the metric $w_B \sim 1 \times 10^{-5}$ cm s^{-1}, where the subscript denotes the value at $z = B$, the top of the bottom boundary layer.

By the relation (28), a value of $w_B \sim 1 \times 10^{-5}$ cm s^{-1} is associated with a vertical diffusivity for density of order $(K_v)_B \sim 1$ cm^2 s^{-1}. Because such small vertical velocities cannot be measured directly, it is this associated vertical diffusivity $(K_v)_B$ which has become a "canonical" value, in the sense of that to which all others should be compared. As discussed in the previous section, most existing determinations of upper bounds for K_v in the upper kilometer of the ocean suggest values of $K_v \sim 0.1$ cm^2 s^{-1}, and the fact that this is considerably smaller than the metric $(K_v)_B$ has come to be considered evidence for the inadequacy of (26) as a local balance. In fact, it may only be evidence for the inadequacy of (27), that is, the vertical advection/diffusion model with *depth independent* w and K_v. This point of view was advanced by Needler (1979) who argued that even if uniform deep upwelling exists, use of (26) in the traditional manner (constant K_v) results in overestimating K_v if $w > 0$ is not constant but increases with depth as predicted by entrainment models of deep water formation (Smith, 1975; Killworth, 1977; Peterson, 1979). Assume then that (26) holds as a *local* balance, but allow w and K_v to be functions of z; then instead of condition (28) we have

$$\frac{w-(K_v)_z}{K_v} = \frac{w+w_d}{K_v} = \frac{\rho_{zz}}{\rho_z} = \frac{1}{b}. \tag{30}$$

Here $w_d \equiv -(K_v)_z$ is the diffusive pseudo-velocity introduced in the discussion of modelling long-term tracer distributions in lakes (Section 3.2, method (i)). In that context, the term involving w_d could be ignored: in the present context, the very slight curvature of deep ocean density profiles requires that the magnitude of the pseudo-advective term be examined carefully. In fact, given the functional form (25) for $K_v(z)$ and the exponential density profile (29), Eq. (30) can be solved for the actual vertical velocity field

$$w(z) = \left(\frac{1}{b} - \frac{w_d}{K_v}\right) K_v = \frac{1}{2}\frac{K_v}{b} = \frac{a_o}{2b} N^{-1}, \tag{31}$$

from which it is apparent that w_d cannot be ignored. The above relation predicts upwelling velocities which decrease upward, as drawn in Figure 9 for the value of $b = 1$ km suitable for the deep North Pacific. The magnitude of w decreases from $\sim 1 \times 10^{-5}$ cm s^{-1} at $z = 1$ km (a depth of 4 km, very near the bottom in the North

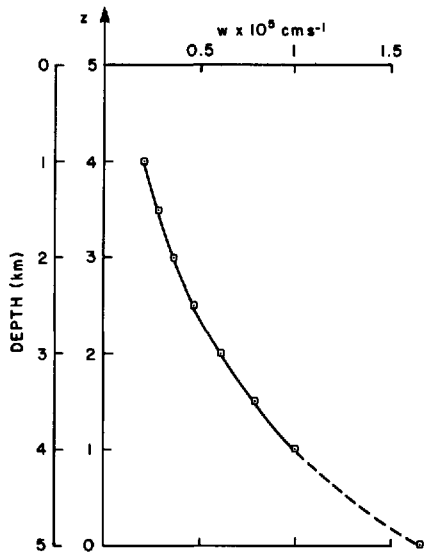

Figure 9. Profile of the vertical velocity $w(z) = K_v(z)/2b$ which would be associated with a vertical eddy diffusivity of the form $K_v(z) = a_o N^{-1}$ *if* an exponential density profile of scale height b is maintained by local balance between upward advection and downward diffusion. Numerical values are calculated with the exponential diffusivity profile of Figure 8: i.e., $a_o = (1 \times 10^{-3})\ \mathrm{cm^2\,s^{-2}}$, $b = 1$ km, and $N = N_o \exp((z - B)/2b)$ with $N_o = 5 \times 10^{-4}\ \mathrm{s^{-1}}$, $B = 1$ km. Note that $\partial w/\partial z < 0$.

Pacific) to $\sim 2 \times 10^{-6}$ cm s^{-1} at $z = 4$ km (near the base of the pycnocline in the subtropical gyre). The latter value is an order of magnitude smaller than that required by diffusive models of the thermocline (e.g., Robinson and Stommel, 1959), a fact consistent with the alternate model of an advective thermocline, as suggested first by Welander (1959), and investigated recently by Jenkins (1980), Rhines and Young (1982) and Luyten *et al.* (1983). This fact also suggests that the path by which bottom water returns to the surface at high latitudes is *not* the main thermocline of the subtropical gyres. This thought was first voiced by Rooth and Ostlund (1972), when considering their estimate of an upper ocean diffusivity $K_v \simeq 0.2\ \mathrm{cm^2\,s^{-1}}$ based on the tritium profile at one station in the Sargasso Sea. They argued that if such low values of *in-situ* vertical diffusivity prove typical of the subtropical gyres, ". . . one cannot escape the conclusion that . . . the return path of the abyssal circulation must be through the polar front regions, rather than through the upper main thermocline." The amount of bottom water formed annually considerably exceeds the amount of water which actually sinks from the surface in polar regions, because turbulent convection cells entrain surrounding fluid as they sink. Thus it is possible that a volume of fluid equal to that which sinks from the surface is returned to the surface annually through the divergent (upwelling) upper-ocean polar fronts, while entrained fluid recirculates

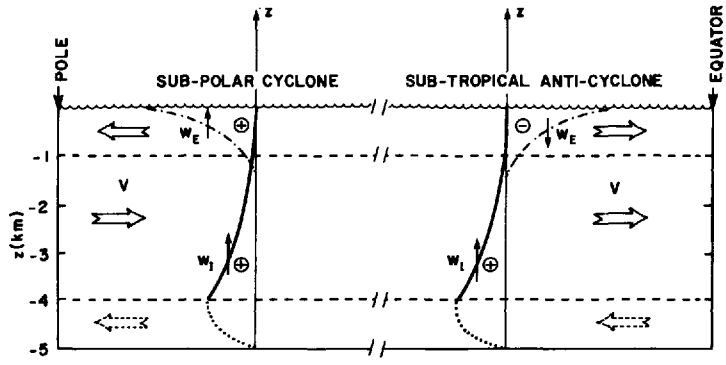

Figure 10. Schematic representation of a proposed field of vertical velocity beneath atmospheric subpolar cyclones and subtropical anticyclones, respectively. Bottom water is supplied to the bottom boundary layer (here assumed to occupy the bottom kilometer of a 5 km deep water column) from which it upwells to balance downward turbulent diffusion of lighter water. Assuming that such a balance holds locally, and using the model of $K_v(z)$ proposed in this paper, the interior vertical velocity w_T is positive and decreases with height above the bottom. In the upper ocean (above 1 km), the vertical velocity field is dominated by Ekman velocities, positive (upward) in regions of Ekman suction within subpolar gyres and negative (downward) in regions of Ekman pumping in subtropical gyres. Simple geostrophic balance requires *equatorward* meridional flow in the interior (large open arrows). By this model, the poleward interior flow of the Stommel-Arons abyssal circulation would be confined to the bottom boundary layer, the only part of the water colum below 1 km depth where $\partial w/\partial z > 0$.

at depth. (Note, however, that the polar fronts may not be the only "holes" in the main thermocline. If meridional flow in the intermediate waters converges toward the equator (see following), the divergent upper-ocean equatorial "front" would be another possible pathway to the near-surface and thence, via western boundary currents, to high latitudes.)

The dynamical consequences of a vertical velocity field which decreases with height are considerable. To the same order of approximation used in the simplified density equation (26), the vorticity equation (22) is unchanged. With $\partial w/\partial z < 0$, the simple geostrophic balance assumed to govern flow in the deep ocean requires that the intermediate waters of the world oceans move *equatorward.* A simple diagram (Fig. 10) illustrates the directions of meridional velocities which result from assuming that the vertical velocity field of the intermediate water (depths between 1 and 4 km) is predominantly the thermohaline-driven field given by (31), while wind-driven Ekman velocities dominate the ocean above ~1 km. (I have drawn the Ekman velocities going to zero at a depth of 1.5 km; this is simply a guess.) In the subtropical gyres, the Ekman velocity is negative so that $\partial w/\partial z < 0$ and the resulting meridional geostrophic velocity is equatorward (large arrows) throughout the water column above the top of some bottom boundary layer (dashed line at 4 km depth). In the subpolar gyres where the Ekman velocity is positive, poleward flow occurs in the upper ocean but the meridional flow in the intermediate water is still equatorward. In this view, poleward motion

required by the Stommel and Arons' model must be confined to the bottom boundary layer, where $\partial w/\partial z > 0$. Although the meridional thermohaline circulation shown in Figure 10 seems somewhat heretical it has certain appealing features. It is compatible with some suggestions that the upper-ocean anticyclonic subtropical gyres, with their predominantly equatorward meridional flows, extend downward in weakened form to abyssal depths. In the Argentine Basin of the southeastern Atlantic, Reid *et al.* (1977) found that "... the circulation of all except the abyssal layer appears to be anticyclonic and so tightly compressed against the western boundary that equatorward flow is observed just offshore of the poleward flow at the boundary," while interpretation of maps of geopotential anomaly for the South Pacific led Reid and Arthur (1975) to conclude that this anticyclonic subtropical gyre extends downward to at least 3 km. Furthermore, equatorward flow in the interior would serve to regularize at least two observational features which are otherwise puzzling.[5] The first is the observed lateral spread of a plume of excess ^{3}He in the South Pacific (Lupton and Craig, 1981). Primordial ^{3}He is contained in warm water leaking from vents at a depth of ~3 km, near 15S along the East Pacific Rise. The water thus tagged ascends to a depth of ~2.5 km, then spreads to the *northwest,* as expected in an anti-cyclonic circulation, rather than to the southeast as expected in a cyclonic circulation such as that of Stommel and Arons. The second feature is existing evidence in water property distributions (Reed, 1969) for an *eastward* flow of deep water along the Aleutian arc in the North Pacific. Warren (1981) labels this ". . . a perplexing feature of the deep circulation," in view of the fact that the poleward interior flow of Stommel and Arons requires a westward return flow along this boundary. However eastward flow would obviously be required to supply an *equatorward* interior flow.

6. Conclusion

The main purpose of this paper has been to examine available observational material relevant to variation of the vertical "eddy" diffusivity K_v with stability, for systems in which diapycnal mixing is thought to be dominated by any one of many forms of internal wave breaking. I have briefly reviewed a recent model (Gargett and Holloway, 1984) which suggests possible forms of such variation, in order to provide a framework for viewing observations from a variety of stratified geophysical systems which may satisfy the associated assumptions. These are (i) fluctuating vertical velocity variances dominated by internal wave motions, (ii) diapycnal mixing initiated at a critical value of a wave-Richardson number and (iii) characterized by a near-constant (small) value of flux Richardson number and (iv) little or no diapycnal flux due to double-diffusive

5. Separate explanations of each feature have recently been advanced (Stommel, 1982; Owens and Warren, 1983)), allowing retention of the Stommel-Arons model if desired. The sole advantage of the present argument is that both features are regularized by the simple assumption that $\partial w/\partial z < 0$ in much of the deep ocean.

processes (this last assumption will be re-examined below). Observational methods of obtaining K_v were examined in considerable detail, and reveal a disagreeable degree of model-dependence inherent to most estimates. The sole unequivocal method, careful use of budgets of conservative scalars in effectively closed basins, suggests the relation

$$K_v = a_o N^{-q}, \text{ with } q \sim 0(1).$$

In the context of the GH model, the value of a_o (unlike q) is system-specific, since it is dependent upon the average rate at which a specific internal wave system is forced.

Whatever values are chosen for q and a_o, the observational evidence clearly supports a functional dependence of K_v upon an *inverse* power of N. At this point, it seems worthwhile to note that this statement can also be made about both of the other two diapycnal mixing mechanisms presently considered for the interior of the stratified ocean, namely boundary mixing and double-diffusion. Armi (1979) has proposed that diapycnal mixing in the deep ocean occurs mainly in turbulent bottom (side) boundary layers, with the effects of such mixing being distributed throughout the interior by isopycnal advection. Assuming the dominance of boundary over interior mixing, and a *zero* vertical velocity field, Armi used a basin-averaged form of the vertical advection/diffusion model of Section 5 and derived a diffusivity $K_v \alpha N^{-2}$. The case of double-diffusive fluxes may be argued more generally (and even more speculatively, since it is not yet clear that an "eddy diffusivity" parameterization will prove acceptable for such processes). Although appropriate "eddy" diffusivities for heat and salt differ, I am concerned only with the net effect on the mass (density) field. Laboratory studies (Huppert and Turner, 1981; Schmitt, 1979) reveal that double-diffusive processes are distinguished by a *counter-gradient* mass flux $F_D \equiv (w'\rho')_D < 0$ which *increases* in magnitude as the vertical stratification ρ_z *decreases:* these features are contained in the general form $F_D \sim -N^{-d}$, $d > 0$. If one wishes to define an "equivalent" eddy diffusivity for density K_D in the usual way, through the relation $F_D = K_D\rho_z$, one obtains $K_D \sim -F_D/\rho_z \sim -N^{-d}/N^2 \sim -N^{-(d+2)}$, a generalized inverse power law dependence upon N. Note that the double-diffusive pseudo-velocity $(-\partial K_D/\partial z < 0)$ is downward rather than the upward diffusive pseudo-velocity $(-\partial K_v/\partial z > 0)$ associated with ordinary (i.e., down-gradient) turbulent fluxes when K_v is a function of z. Since double-diffusive processes occur only in those parts of the water column where vertical gradients of T and S have the same sign, their associated density fluxes may contribute considerable vertical structure to a *net* vertical diffusive pseudo-velocity, $-\partial (K_v + K_D)/\partial z$.

In Section 4, I have re-visited a simple model of the maintenance of the deep-ocean density field, primarily to demonstrate that the diffusive pseudo-velocities associated with a depth (more properly, N) dependent K_v may be comparable to previous estimates of the true vertical velocity. As cautioned by Stommel and Arons (1960b), any change in the parametric formulation of vertical mixing in the ocean can have

considerable *dynamical* effect (unlike lateral mixing: while K_H values of the order 10^7–10^8 cm^2 s^{-1} have a marked effect on tracer distributions, they produce negligible effect on the dynamics of the basic flow (Stommel and Aarons, 1960b)). A more complete theory will parameterize K_v in terms of N and derive *both* w and ρ fields from the equations of motion and boundary conditions, (rather than assume a form for $\rho(z)$ in order to solve for $w(z)$ as done here) such a system, subject to some restrictions on possible boundary conditions, is being explored by Young and Ierley (W. R. Young, pers. comm., 1983). The present speculation on the meridional circulation which might be associated with the form $K_v = a_o N^{-1}$ is justified only by the degree to which qualitative features agree with various observations, and by the interesting suggestion that we may not yet know even the *direction* of the thermohaline circulation in much of the ocean interior.

Acknowledgments. I would like to thank a number of referees, of both this paper and a previous draft, for their helpful comments. I am grateful also to Sus Tabata, Sarilee Anderson and Joe Reid, who helped me assemble the estimates of N in Figure 8. This paper was originally written during a visit to the School of Oceanography, University of Washington and re-written during a stay at the Institute of Geophysics and Planetary Physics, Scripps Institution of Oceanography. I thank colleagues at both places for their hospitality as well as their stimulating comments.

REFERENCES

Armi, L. 1979. Effects of variations in eddy diffusivity on property distributions in the oceans. J. Mar. Res. *37,* 515–530.

Armi, L. and D. B. Haidvogel. 1982. Effects of variable and anisotropic diffusivities in a steady-state diffusion model. J. Phys. Oceanogr., *12,* 785–794.

Batchelor, G. K. 1959. Small scale variation of convected quantities like temperature in turbulent fluid. J. Fluid Mech., *5,* 113–133.

Caldwell, D. R. 1983. Small-scale physics of the ocean. Rev. Geophys. Space Phys., *21,* 1192–1205.

Caldwell, D. R., T. M. Dillon, J. M. Brubaker, P. A. Newberger and C. A. Paulson. 1980. The scaling of vertical temperature gradient spectra. J. Geophys. Res., *85,* 1917–1924.

Carmack, E. C. and T. D. Foster. 1975. On the flow of water out of the Weddell Sea. Deep-Sea Res., *22,* 711–724.

Chung, Y. 1975. Areal extent of the benthic front and variation of scale height in Pacific Deep and Bottom Waters. J. Geophys. Res., *80,* 4169–4178.

Craig, H. 1969. Abyssal carbon and radiocarbon in the Pacific. J. Geophys. Res., *74,* 5491–5506.

Danish Hydraulic Institute (DANSK HYDRAULISK INSTITUT (DHI)). 1979. Marmorilik Hydrografiske Undersogelser 1978. Greenex A/S. Horsholm, 104 pp.

Dillon, T. M. and D. R. Caldwell. 1980. The Batchelor spectrum and dissipation in the upper ocean. J. Geophys. Res., *85,* 1910–1916.

Fiadeiro, M. E. 1982. Three-dimensional modeling of tracers in the deep Pacific Ocean: II. Radiocarbon and the circulation. J. Mar. Res., *40,* 537–550.

Fiadeiro, M. E. and H. Craig. 1978. Three-dimensional modeling of tracers in the deep Pacific Ocean: I. Salinity and oxygen. J. Mar. Res., *36,* 323–355.

Gammon, R. H., J. Cline and D. Wisegarver. 1982. Chlorofluoromethanes in the northeast Pacific Ocean: measured vertical distributions and application as transient tracers of upper ocean mixing. J. Geophys. Res., *87,* 9441–9454.

Gargett, A. E. 1976. An investigation of the occurrence of oceanic turbulence with respect to finestructure. J. Phys. Oceanogr., *6,* 139–156.

Gargett, A. E. and G. Holloway. 1984. Dissipation and diffusion by internal wave breaking. J. Mar. Res., *42,* 15–27.

Gargett, A. E. and T. R. Osborn. 1981. Small-scale shear measurements during the Fine and Microstructure Experiment (FAME). J. Geophys. Res., *86,* 1929–1944.

Gargett, A. E., T. R. Osborn and P. W. Nasmyth. 1984. Local isotropy and the decay of turbulence in a stratified fluid. J. Fluid Mech., (submitted).

Garrett, C. 1979. Mixing in the ocean interior. Dyn. Atmos. Oceans, *3,* 239–265.

Garrett, C. J. R. and W. Munk. 1972. Space-time scales of internal waves. Geophys. Fluid Dyn., *2,* 225–264.

Gibson, C. H. 1981. Buoyancy effects in turbulent mixing: sampling turbulence in the stratified ocean. Amer. Inst. of Aero. and Astro. Journal, Proceedings of AIAA 13th Fluid and Plasma Dynamics Conference, 1980, *19,* 1394–1400.

—— 1980. Fossil temperature, salinity and vorticity turbulence in the ocean, *in* Marine Turbulence, J. C. J. Nihoul, ed., Elsevier Series, *28,* 221–258.

Gibson, C. H. and W. H. Schwartz. 1963. The universal equilibrium spectra of turbulent velocity and scalar fields. J. Fluid Mech., *16,* 365–384.

Gregg, M. C. 1980. Microstructure patches in the thermocline. J. Phys. Oceanogr., *10,* 915–943.

—— 1977. Variations on the intensity of small-scale mixing in the main thermocline. J. Phys. Oceanogr., *7,* 436–454.

—— 1976. Finestructure and microstructure observations during the passage of a mild storm. J. Phys. Oceanogr., *6,* 528–555.

Gregg, M. C. and M. G. Briscoe. 1979. Internal waves, finestructure, microstructure, and mixing in the ocean. Rev. Geophys. Space Phys., *17,* 1524–1548.

Hogg, N., P. Biscaye, W. Gardner and W. J. Schmitz, Jr. 1982. On the transport and modification of Antarctic Bottom Water in the Vema Channel. J. Mar. Res., *40* (Suppl)., 231–263.

Holloway, G. 1983. A conjecture relating oceanic internal waves and small-scale processes. Atmos.-Oceans, *21,* 107–122.

Huppert, H. E. and J. S. Turner. 1981. Double-diffusive convection. J. Fluid Mech., *106,* 299–329.

Jassby, A. and T. Powell. 1975. Vertical patterns of eddy diffusion during stratification in Castle Lake, California. Limnol. Oceanogr., *20,* 530–543.

Jenkins, W. J. 1980. Tritium and ^{3}He in the Sargasso Sea. J. Mar. Res., *38,* 533–569.

Killworth, P. D. 1977. Mixing on the Weddell Sea continental slope. Deep-Sea Res., *24,* 427–448.

Kullenberg, G. 1974. Investigation of small-scale vertical mixing in relation to the temperature structure in stably stratified waters. Adv. Geophys., *18A,* 339–351.

Kuo, H. H. and G. Veronis. 1973. The use of oxygen as a test for an abyssal circulation model. Deep-Sea Res., *20,* 871–888.

Lewis, E. L. and R. G. Perkin. 1982. Seasonal mixing processes in an Arctic fjord system. J. Phys. Oceanogr., *12,* 74–83.

Li, Y.-H. 1973. Vertical eddy diffusion coefficient in Lake Zurich. Schweiz. Z. Hydrol., *35,* 1–7.

Lietzke, T. A. and A. Lerman. 1975. Effects of bottom relief in two-dimensional oceanic eddy diffusion models. Earth Planet. Sci. Letters, *24,* 337–344.

Lueck, R. G., W. R. Crawford and T. R. Osborn. 1983. Turbulent dissipation over the continental slope off Vancouver Island. J. Phys. Oceanogr., *13,* 1809–1818.

Lupton, J. E. and H. Craig. 1981. A major Helium-3 source at 15S on the East Pacific Rise. Science, *214,* 13–18.

Luyten, J. R., J. Pedlosky and H. Stommel. 1983. The ventilated thermocline. J. Phys. Oceanogr., *13,* 292–309.

Monin, A. S. and A. M. Yaglom. 1971. Statistical Fluid Mechanics, Vol. 1, MIT Press, Cambridge, MA, *733* pp.

Munk, W. H. 1966. Abyssal recipes. Deep-Sea Res., *13,* 707–730.

—— 1981. Internal waves and small-scale processes, *in* Evolution of Physical Oceanography, Scientific Papers in Honor of Henry Stommel, B.A. Warren and C. Wunsch, eds., MIT Press, 264–291.

Needler, G. T. 1979. Comments on high-latitude processes for ocean climate modeling. Dyn. Atmos. Oceans, *3,* 231–237.

Oakey, N. S. 1982. Determination of the rate of dissipation of turbulent energy from simultaneous temperature and velocity shear microstructure measurements. J. Phys. Oceanogr., *12,* 256–271.

Oakey, N. S. and J. A. Elliott. 1977. Vertical temperature gradient structure across the Gulf Stream. J. Geophys. Res. *82,* 1369–1380.

Osborn, T. R. and C. S. Cox. 1972. Oceanic fine structure. Geophys. Fluid Dyn., *3,* 321–345.

Osborn, T. R. and W. R. Crawford. 1980. An airfoil probe for measuring velocity fluctuations in water, *in* Air-Sea Interaction: Instruments and Methods, F. Dobson, L. Hasse and R. Davis, eds., Plenum, N.Y., 801 pp.

Owens, W. B. and B. A. Warren. 1982. Deep northern boundary currents in the North Pacific. EOS, Trans. Amer. Geophys. Union, *64,* 730 (Abstract).

Peterson, W. H. 1979. A steady thermohaline convection model. Tech. Rep. TR-79-4, University of Miami, Ph.D. thesis, 160 pp.

Quay, P. D., W. S. Broecker, R. H. Hesslein and D. W. Schindler. 1980. Vertical diffusion rates determined by tritium tracer experiments in the thermocline and hypolimnion of two lakes. Limnol. Oceanogr., *25,* 201–218.

Reed, R. K. 1969. Deep water properties and flow in the central North Pacific. J. Mar. Res., *27,* 24–31.

Reid, J. L. and R. S. Arthur. 1975. Interpretation of maps of geopotential anomaly for the deep Pacific Ocean. J. Mar. Res., *33* (Suppl.), 37–52.

Reid, J. L., W. D. Nowlin and W. C. Patzert. 1977. On the characteristics and circulation of the southwestern Atlantic Ocean. J. Phys. Oceanogr., *7,* 62–91.

Rhines, P. and W. R. Young. 1982. A theory of wind-driven ocean circulation. I. Mid-ocean gyres. J. Mar. Res., *40,* (Suppl.), 559–596.

Robinson, A. and H. Stommel. 1959. The oceanic thermocline and the associated thermohaline circulation. Tellus, *11,* 295–308.

Rooth, C. and H. G. Ostlund. 1972. Penetration of tritium into the Atlantic thermocline. Deep-Sea Res., *19,* 481–492.

Sarmiento, J. L. and C. G. H. Rooth. 1980. A comparison of vertical and isopycnal mixing models in the deep sea based on Radon 222 measurements. J. Geophys. Res., *85,* 1515–1518.

Schmitt, R. W., Jr. 1979. Flux measurements on salt fingers at an interface. J. Mar. Res., *37,* 419–436.

Smethie, W. M., Jr. 1980. Estimation of vertical mixing rates in fjords using naturally occurring Radon-222 and salinity as tracers, *in* Fjord Oceanography, H. J. Freeland, D. M. Farmer and C. D. Levings, eds., Plenum Press, N.Y., 241–249.

Smith, P. C. 1975. A streamtube model for bottom boundary currents in the ocean. Deep-Sea Res., *22,* 853–873.

Stommel, H. 1982. Is the South Pacific helium-3 plume dynamically active? Earth Planet. Sci. Letters, *61,* 63–67.

—— 1958. The abyssal circulation. Deep-Sea Res., *5,* 80–82.

Stommel, H. and A. B. Arons. 1960a. On the abyssal circulation of the world ocean—I Stationary planetary flow patterns on a sphere. Deep-Sea Res., *6,* 140–154.

—— 1960b. On the abyssal circulation of the world ocean—II An idealized model of the circulation pattern and amplitude in oceanic basins. Deep-Sea Res., *6,* 217–233.

Svensson, T. 1980. Tracer measurement of mixing in the deep water of a small stratified sill fjord, *in* Fjord Oceanography. H. J. Freeland, D. M. Farmer and C. D. Levings, eds., Plenum Press, N.Y., 233–240.

Tennekes, H. and J. L. Lumley. 1972. A First Course in Turbulence. The MIT Press, Cambridge, MA, 300 pp.

Warren, B. A. 1977. Shapes of deep density-depth curves. J. Phys. Oceanogr., *7,* 338–344.

—— 1981. Deep circulation of the world ocean, *in* Evolution of Physical Oceanography, B. A. Warren and C. Wunsch, eds., MIT Press, Cambridge, MA, 623 pp.

Washburn, L. and C. H. Gibson. 1982. Measurements of oceanic temperature microstructure using a small conductivity sensor. J. Geophys. Res., *87,* 4230–4240.

Welander, Pierre. 1959. An advective model of the ocean thermocline. Tellus, *11,* 309–318.

Whitehead, J. A., Jr. and L. V. Worthington. 1982. The flux and mixing rates of Antarctic Bottom Water within the North Atlantic. J. Geophys. Res., *87,* 7903–7924.

Worthington, L. V. 1969. An attempt to measure the volume transport of Norwegian Sea overflow water through the Denmark Strait. Deep-Sea Res., *16* (Suppl.), 421–432.

Wyrtki, K. 1961. The thermohaline circulation in relation to the general circulation in the oceans. Deep-Sea Res., *8,* 39–64.

Received: *11 August, 1983;* revised: *6 January, 1984.*